Sentinel-1 Synthetic Aperture Radar Burned Area Detection Using Expectation Maximization in a Multiscale Approach

A Thesis submitted in partial fulfillment of the requirements for the degree of Master of Science at George Mason University

by

Louis D. Heying
Bachelor of Science
Towson University, 2014

Director: Ruixin Yang, Associate Professor
Geography and Geoinformation Science Department

Spring Semester2023
George Mason University
Fairfax, VA

DEDICATION

I dedicate this work to my father and mother, Donald and Mary, and to my sister, Ruthie, and my brother, John.

ACKNOWLEDGEMENTS

I wish to thank my advisor, Dr. Ruixin Yang, for his guidance and support throughout this process. I also want to thank the members of my committee for their invaluable input and patience: Dr. John Qu, and Dr. Donglian Sun. I would also like to thank my family, friends, and colleagues for supporting and believing in me as I worked through this thesis, particularly both friend and colleague, Kyle Foster; and former Geography Club President and friend David M. Finally, I wish to thank the Alaska Satellite Facility for providing the code for the methodology that this work builds upon. This work was not supported by any funding and does not represent the views of the United States Government.

TABLE OF CONTENTS

LIST OF TABLES

LIST OF FIGURES

LIST OF ABBREVIATIONS

Advanced Very High Resolution Radiometer ....AVHRR
Alaska Satellite Facility .... ASF
Application Programming Interface .... API
Decibel ....dB
differenced Normalized Burn Ratio... dNBR
Digital Elevation Model...DEM
European Space Agency ....ESA
Google Earth Engine..GEE
Ground Range Detected...GRD
Hybrid Pluggable Processing Pipeline... HyP3
Indian Space Research Organisation .... ISRO
Intergovernmental Panel on Climate Change ....IPCC
Moderate Resolution Imaging Spectroradiometer ....MODIS
National Aeronautics and Space Administration...NASA
NASA-ISRO Synthetic Aperture Radar ....NISAR
Near Infrared..NIR
Normalized Burn Ratio .... NBR
Representative Concentration Pathway ....RCP
Shortwave Infrared..SWIR
Shuttle Radar Topography Mission ....SRTM
Single Look Complex .... SLC
Sum of Square Error ....SSE
Synthetic Aperture Radar..SAR
Vertical transmit Vertical receive VV
Vertical transmit Horizontal receive..VH
3D Elevation Program...3DEP

ABSTRACT

SENTINEL-1 SYNTHETIC APERTURE RADAR BURNED AREA DETECTION USING EXPECTATION MAXIMIZATION IN A MULTISCALE APPROACH

Louis D. Heying, M.S.

George Mason University, 2023

Thesis Director: Dr. Ruixin Yang

This research explores wildfire burn mapping using Sentinel-1 Synthetic Aperture Radar (SAR) imagery for the 2021 Woods Creek Fire in the Helena-Lewis and Clark National Forest in Montana and the 2021 French Fire near Lake Isabella in Kern County California. Sentinel-1 SAR imagery is used since it can be collected during most weather conditions as well as in heavy smoke and is useful in the upper latitudes where wildfires often occur. Both the ascending and descending orbits as well as the co-polarity (VV) and cross-polarity (VH) are evaluated. The increase of wildfire occurrence is the result of lower precipitation and fuel moisture content as a result of climate change. The methodology by which SAR imagery detects wildfire burns is adapted to use SAR imagery from Google Earth Engine (GEE) and a method provided by the Alaska Satellite Facility (ASF). This method utilizes a stationary wavelet transform and math morphology to process imagery at various scales and expectation maximization in order to generate

change classes. The resulting burn area is compared to Sentinel-2 differenced Normalized Burn Area (dNBR) and MODIS Burned Area. The ascending orbits of Sentinel-1 burned areas provided the best results compared to those of the descending orbits likely due to the limited ability of GEE to radiometrically terrain correct SAR imagery.

I. INTRODUCTION

Wildfires in North America are intensifying and becoming more commonplace as a result of the warming effects of climate change with the number of wildfires having increased in the late twentieth century and into the twenty-first century (Abatzoglou and William 2016, Parks and Abatzoglou 2020). These gradual changes have resulted in extended and extreme summer conditions which can lead to a greater abundance of fuel (Williams et al. 2019). Higher temperatures and lower precipitation have increased the frequency of hydrologic drought which contribute to this abundance of fuel comprised mostly of organic material (Trenberth 2011, Littell et al. 2016). Reduced snowpack, particularly in the North American West, is an additional contributor to the increases in burn fuel. There is an enhanced tendency to experience rain rather than snow during the winter season, which has adverse effects in the summer (Trenberth 2011). Drier conditions are not the sole explainer of climate change which leads to more frequent wildfires as fuel or vegetation type also have an impact on fire regimes (McKenzie and Littell 2017). At the same time, the summer season is lengthening at higher latitudes which is consequential to increased drought conditions through decreased snowpack (Schwartz 1998, Jolly et al. 2015). Earlier snowmelt in the North American West additionally contributes to increased wildfire activity (Westerling 2016). Particularly, these conditions contribute to lower fuel moisture and results in a longer fire season (Halofsky et al. 2020).

Frequent wildfire impacts not only the ecologic balance of the forests it occurs in, but also has societal and economic impact in the populated areas which border forests (Keeton et al. 2007, Ager et al. 2019). Additionally, one of the outcomes of increased agriculture around the world is that the amount of burned area has decreased despite the increase in fire frequency (Andela et al. 2017).

With the increasing frequency of wildfire, forests are subject to repeated fires which impact the diversity of the forest as well as how quickly the forest recovers (Halofsky et al. 2020). The Representative Concentration Pathway (RCP) are trajectory scenarios for greenhouse gas projections where RCP 4.5 is an intermediate scenario where emissions level off and decline after 2040 and RCP 8.5 is an extreme scenario where emissions continue to increase. Viewing wildfire through the lens of the Intergovernmental Panel on Climate Change (IPCC) assessments, future projections utilizing climate models indicate that wildfires will further increase both under the RCP 4.5 and RCP 8.5 climate scenarios (Gao et al. 2021). This is further supported by climate projections which show that North America will be at an exceptional risk of drought through the twenty-first century (Cook et al. 2015). Increases in wildfire frequency as a result of climate change will not only occur during the summer season but also during the winter season in which fire activity had previously been minimal in the North America (Heidari et al. 2021). In November 2018, the non-summer Camp Fire in California was the deadliest and one of the costliest in the state’s history underscoring the risk of wildfire in the current century costing over $16 billion and resulting in the loss of 85 lives (Baldassari 2018, CNBC 2018).

Wildfires are an ever-increasing threat for forests throughout the world, and especially for forests of North America. Accurate estimates of wildfire burn are difficult with in situ measurements due to the risks associated, and therefore, remote sensing is commonly used to estimate total area impacted. However, often times optical imagery is unable to obtain a clear observation during a wildfire event due to impacts of weather, time of day, or smoke. The microwave capabilities of SAR imagery are not dependent on illumination from the Sun but from the sensor itself and can thus be utilized under most conditions. SAR sensors are becoming more prolific as a source of remotely sensed imagery with various commercial SAR constellations entering into orbit as well as civil SAR sensors such as the upcoming National Aeronautics and Space Administration (NASA) and the Indian Space Research Organisation (ISRO) collaborative satellite NISAR (NASA-ISRO Synthetic Aperture Radar) to be launched into orbit in 2024. Radar sensors operate at various radio frequencies and bandwidths which interact with materials differently. This satellite will have an L-band sensor which is advantageous for monitoring forests. In advance of the launch of NISAR and the availability of its data, it is necessary to use more readily available C-band imagery. The L-band range of frequencies is from 1.0-2.0 gigahertz while the C-band rage of frequencies is from 4.0-8.0 gigahertz. This study intends to look at a method utilized by the Alaska Satellite Facility (ASF) using C-band SAR that is currently available through the European Space Agency’s (ESA) Copernicus Programme and to apply this method to a sample of wildfires in North America. The specific wildfires in this study are in areas which have a wide variety of terrain and therefore a method to mitigate radar effects from terrain is used. Many wildfires occur in areas which may not always be ideal for SAR imagery and using terrain correction techniques are required in order to get an accurate observation of a region.

In the past, wildfire burns have been typically mapped using remotely sensed optical imagery. The Landsat missions have been a mainstay of the mid to high resolution remotely sensed data from space since the 1970s and has been joined by the European Space Agency's (ESA) Copernicus Programme Sentinel-2 multispectral sensor. Observation by these sensors is hampered at higher latitudes by cloud cover as well as interference from the thick smoke from wildfires thus limiting the amount of usable data. The Normalized Difference Vegetation Index (NDVI) has been previously used to map out wildfire burn areas where there has been an abundance of vegetation using both the Advanced Very High Resolution Radiometer (AVHRR) and Landsat (Kasischke et al. 1993, Viedma et al. 1997, Salvador et al. 2000). One of the typical methods of mapping wildfire is through the use of the differenced Normalized Burn Ratio (dNBR) which calculates the change in what can be considered burn area between pre-fire and post-fire imagery (Garcia and Caselles 1991, Cocke et al. 2005, Key and Benson 2006). This method originally used Landsat Near-Infrared (NIR) and Shortwave-Infrared (SWIR) bands, around 7.5-9.0 micrometers and 2.08-2.35 micrometers respectively, to highlight burn based on decreases in plant moisture and increases in ground reflectivity (Garcia and Caselles 1991, Cocke et al. 2005, Key and Benson 2006).

Observations of Earth's surface can be made under most weather conditions through the use of ESA's Sentinel-1 Synthetic Aperture Radar (SAR) constellation. The Sentinel-1 constellation provides SAR imagery that can be used to study environmental phenomena such as agriculture and change detection over a set observation scenario—six or twelve days depending on the region of the world (Fletcher et al. 2012, ESA 2012). Sentinel-1 has been collecting data since October 2014 and is able to collect texture and surface information in the form of phase and amplitude data (Fletcher et al. 2012, ESA 2012). The C-band sensor on the Sentinel-1 satellites collects dual polarity SAR imagery in the co-polarity (VV or HH) and the cross-polarity (VH or HV). A visual example of the relationship between the VV and VH polarities can be seen in Figure 1 as false color composite. The utilization of SAR imagery allows for an additional method to monitor wildfire burns in cloudier regions of the world. The research question for this thesis is to apply the multiscale approach for detecting change in Sentinel-1 images and apply it to a sample of wildfires in North America.

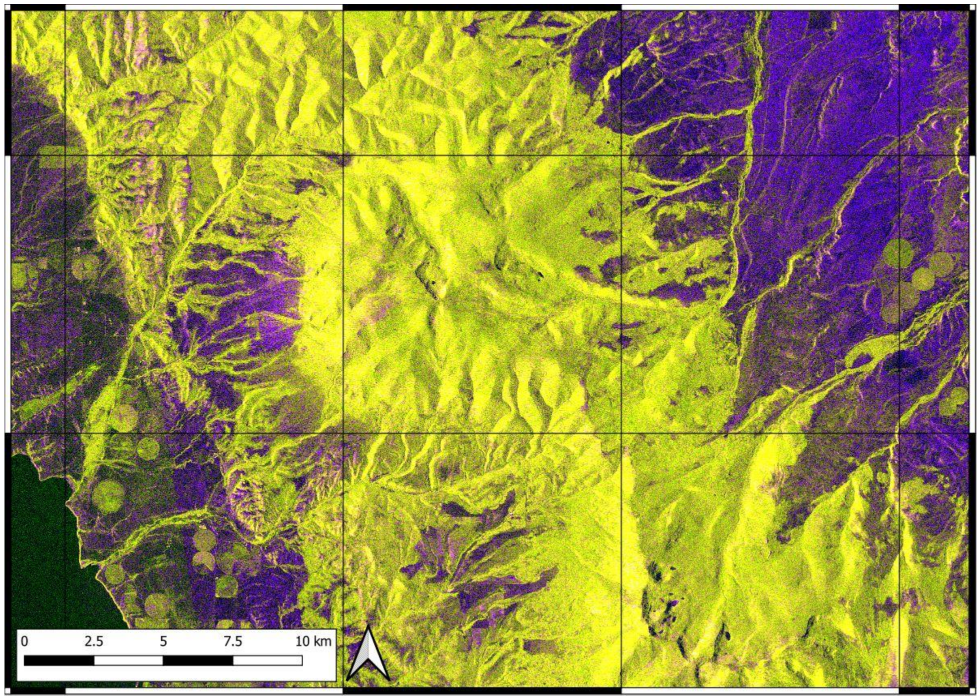

Figure 1. Colorized Sentinel-1 SAR image over the location of the Woods Creek Fire dated August 8, 2021. The colorized image is an RGB composite of the VV, VH and VV/VH ratio after conversion to dB.

II. DATA COLLECTION

C-Band SAR can be used to observe the change in scattering from vegetation comparing before and after a fire event (Imperatore et al. 2017). The mechanism by which SAR interacts with vegetation is both geometric and dielectric which depends on the vegetation type and the nature of the wildfire (Imperatore et al. 2017). Previous studies found that C-Band and L-Band SAR gave the best results for forest monitoring due to the lower frequency of transmission interacting with the leaves in the forest canopy and tree trunks (Tanase et al. 2010). In this particular case, vegetation is able to be considered a dielectric for the radar energy based on the water content of the vegetation (Steele-Dunne et al. 2017). Using Sentinel-1 C-Band SAR, a decrease in cross-polarity (VH) radar backscatter—energy returning back to the satellite—can be used to observe effects of vegetation burn, while an increase in the co-polarity (VV) radar backscatter can be used to look at the secondary effects of a wildfire burn which includes increased exposure of the ground or a double bounce effect (Imperatore et al. 2017). This effect would be seen when the leafy vegetation is burned away which changes the scattering effect of radar energy to react multiple times with the woody structure of vegetation before returning to the sensor.

The first event used for this study is the Woods Creek Fire in the Helena-Lewis and Clark National Forest in Montana, United States. The wildfire is located about 16 miles from Townsend, Montana and began on July 19, 2021 and was fully contained by October 31, 2021. This site was selected as it is a higher latitude—above 45°N— wildfire event in North America and is in a region of mountainous terrain where many wildfires often occur (See Figure 2). Sentinel-1 SAR and Sentinel-2 multispectral data are available in this area. The Sentinel-1 images are dated before the fire and after it had started. Several ratio images will be created to look at the progress of the fire over time for both the co-polarity (VV) and the cross-polarity (VH) with the reference image dated July 3, 2021. The location of Woods Creek Fire is displayed in Figure 2 along with the French Fire in California. A total of six ratio images for both orbit directions will be created; for each of the three comparison dates, one for the co-polarity and the other for the cross-polarity image.

The second study area is the French Fire which occurred in California from August 18, 2021 through October 21, 2021. This fire occurred near Lake Isabella in Kern County, California (see Figure 2). The area exhibits a moderate amount of terrain and thus terrain correction is necessary as well though is not considered high latitude. These two fires were selected in order to evaluate the overall methodology on a diverse subset of locations.

All of the images are accessible in Google Earth Engine (GEE) before being downloaded to be further processed in a Python environment. For the Woods Creek Fire, the images being used in the ascending orbit using relative orbit number 164. Due to the terrain, the ascending orbit may be impacted by terrain despite methods in GEE to correct for slope. A descending orbit will be investigated as well using relative orbit number 100 and a reference image dated July 7, 2021. A list of these images can be found in Table 1.

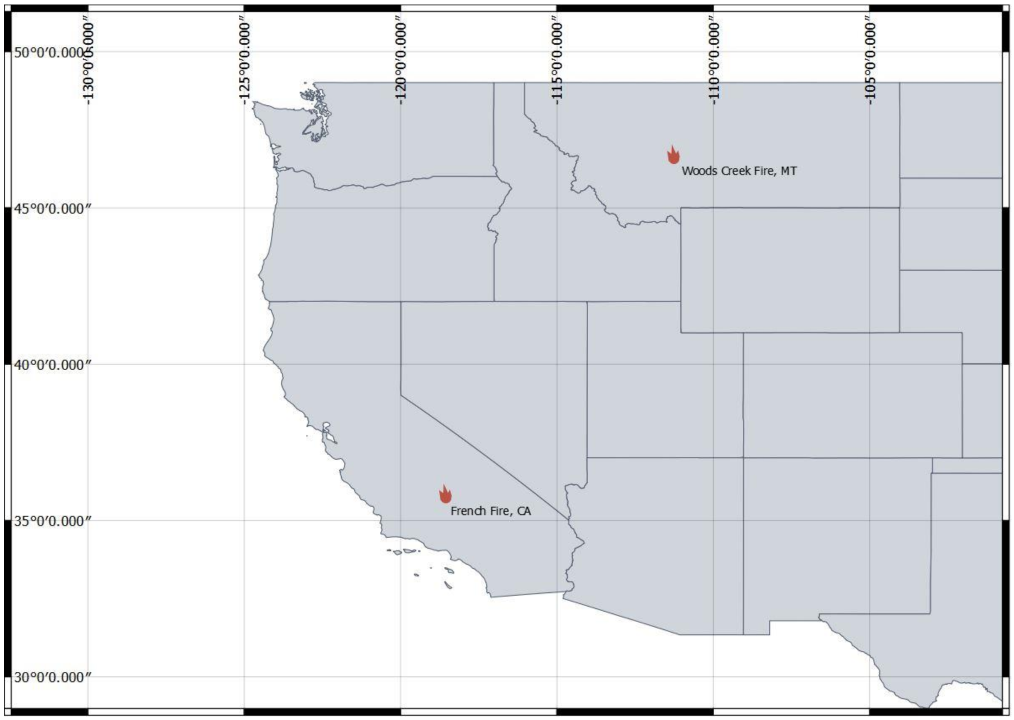

Figure 2. Overview of wildfire locations for this study in the United States.

The Sentinel-1 images used for the French Fire were from relative orbit number 64 for the ascending pass and relative orbit number 144 for the descending pass (See Table 2). The reference images to create the ratio images for the descending and ascending orbit are dated August 15, 2021 and August 4, 2021 respectively. Again, a total of six ratio images for each orbit direction will be looked at for the French Fire.

Table 1. List of the images from the Ascending and Descending orbits and the corresponding date for the Woods Creek Fire. The fire began on July 19, 2021 and was contained on October 31, 2021. The entries in bold font are used a corresponding reference images for the ratio images.

Ascending Orbit Image Name at the Woods Creek Fire	**Date**
S1B_IW_GRDH_1SDV_20210703T012005_20210703T012030_027623_034C01_8499	**7/3/2021**
S1B_IW_GRDH_1SDV_20210808T012007_20210808T012032_028148_035BA1_81AC	8/8/2021
S1B_IW_GRDH_1SDV_20210913T012009_20210913T012034_028673_036BFE_937C	9/13/2021
S1B_IW_GRDH_1SDV_20211007T012009_20211007T012034_029023_037695_7565	10/7/2021
Descending Orbit Image Name at the Woods Creek Fire	**Date**
S1A_IW_GRDH_1SDV_20210707T133234_20210707T133259_038672_04904A_5D62	**7/7/2021**
S1A_IW_GRDH_1SDV_20210812T133236_20210812T133301_039197_04A082_87AC	8/12/2021
S1A_IW_GRDH_1SDV_20210917T133237_20210917T133302_039722_04B28B_4E0	9/17/2021
S1A_IW_GRDH_1SDV_20211011T133238_20211011T133303_040072_04BE95_AFFB	10/11/2021

The difference between the ascending and descending orbits is the direction by which the data are collected by the Sentinel-1 satellites and may impact the observed data in areas of high terrain with radar shadow or void areas. The satellites collect data at a 29.1° - 46.0° incidence angle— which is measured from the angle of the zenith to the sensor—depending on the position of the ground in relation to the satellite—which does not account for the slope of the terrain. The co- and cross polarities will also be processed for the ascending and descending orbit images. The SAR imagery format utilized is the Ground Range Detected (GRD) imagery since this is stored in the GEE catalog as opposed to the Single Look Complex imagery (SLC).

Table 2. List of the images from the Descending and Ascending orbit and the corresponding date for the French Fire. The fire began on August 18, 2021 and was contained on October 21, 2021. The entries in bold font are used as the corresponding reference images for the ratio images.

Descending Orbit Image Name at the French Fire	Date
S1A_IW_GRDH_1SDV_20210815T140015_20210815T140040_039241_04A1FD_BACF	**8/15/2021**
S1A_IW_GRDH_1SDV_20210827T140016_20210827T140041_039416_04A7FC_D64B	8/27/2021
S1A_IW_GRDH_1SDV_20210920T140017_20210920T140042_039766_04B3FD_F79E	9/20/2021
S1A_IW_GRDH_1SDV_20211026T140017_20211026T140042_040291_04C632_E950	10/26/2021
Ascending Orbit Image Name at the French Fire	Date
S1B_IW_GRDH_1SDV_20210804T015014_20210804T015039_028090_0359D6_362B	**8/4/2021**
S1B_IW_GRDH_1SDV_20210828T015015_20210828T015040_028440_0364BA_6D6E	8/28/2021
S1B_IW_GRDH_1SDV_20210921T015016_20210921T015041_028790_036F96_0332	9/21/2021
S1B_IW_GRDH_1SDV_20211027T015017_20211027T015042_029315_037FA6_5A1E	10/27/2021

Sentinel-2 multispectral imagery will also be used for the accuracy assessment of the SAR product. This data will also be accessed via GEE where it has been already preprocessed for surface reflectance under the Sentinel-2 Level 2A Surface Reflectance image collection. This data will be used to generate the dNBR for the fires at a 20-meter resolution (See Table 3). The Sentinel-2 based reference images for the dNBR are dated July 24, 2021 for the Woods Creek Fire and August 1, 2021 for the French Fire.

Table 3. List of Sentinel-2 images to be used for dNBR for the Woods Creek Fire and the French Fire. The entries in bold font are used a corresponding reference images for the dNBR.

Sentinel-2 Images for Woods Creek Fire	**Date**
S2B_MSIL2A_20210724T181919_N0301_R127_T12TVS_20210724T210835	*7/24/2021*
S2B_MSIL2A_20210813T181919_N0301_R127_T12TVS_20210813T211107	8/13/2021
S2B_MSIL2A_20210912T181909_N0301_R127_T12TVS_20210912T222650	9/12/2021
S2B_MSIL2A_20211002T182109_N0301_R127_T12TVS_20211002T222829	10/2/2021
Sentinel-2 Images for French Fire	**Date**
S2A_MSIL2A_20210801T182921_N0301_R027_T11SLV_20210801T224704	*8/1/2021*
S2B_MSIL2A_20210826T182919_N0301_R027_T11SLV_20210826T222949	8/26/2021
S2A_MSIL2A_20210920T183041_N0301_R027_T11SLV_20210920T230838	9/20/2021
S2B_MSIL2A_20211028T184509_N0301_R070_T11SLV_20211028T211942	10/28/2021

The Moderate Resolution Imaging Spectroradiometer (MODIS) Burned Area which is also found in the GEE catalog was used to check against the SAR areas as well (Giglio et al. 2021). The MODIS Burned Area dataset is at a resolution of 500 meters and combines data from the Aqua and Terra MODIS sensors. The data are stored as monthly composites with burned by Julian day The dates that were used for the burn area were the dates of August 12, 2021 and the maximum burn area date of September 17, 2021 for the Woods Creek Fire in Montana and the date of August 28, 2021 and the maximum burn area date of September 21, 2021 for the French Fire in California.

Other methods of wildfire burn extraction that have previously been utilized include using SAR interferometric methods to look at coherence in a burn area between two dates and using a ratio or difference image of two time periods and using thresholding methods (Liew et al. 1999, Lasaponara and Tucci 2019). One of the thresholding methods often used is K-Means which looks for clusters of data points on a histogram (Celik 2009, Lee et al. 2021). Some additional methods use a data fusion approach in which optical imagery is used in combination with SAR imagery and processed through a neural network (Ban et al. 2020, Zhang et al. 2019, Zhang et al. 2021).

III. METHODOLOGY

The methodology in use first utilizes images in the Google Earth Engine (GEE) catalog before further processing takes places. GEE is a multi-petabyte platform which contains various satellite imagery and geospatial datasets. It allows for rapid prototyping and image processing on Google's Cloud infrastructure as a result of its all-in-one web interface and Python and JavaScript APIs (Gorelick et al. 2017). The Sentinel-1 SAR data in GEE has been preprocessed to include thermal noise removal, radiometric calibration, and has been slope corrected. The benefit of using GEE is that the data has been preprocessed up to a certain point which enables the user to tailor the data to their needs. Further preprocessing will be done through another GEE tool, the Analysis Ready Data Preparation toolkit for Sentinel-1 which is a series of tools that provides additional preprocessing for Sentinel-1 imagery in GEE (Mullissa et al. 2021). The toolkit provides additional terrain flattening for Sentinel-1 SAR imagery. An acknowledged drawback of this type terrain flattening utilized within GEE is that without precise orbit data, the results still suffer from passive distortions such as layover and shadow. The preprocessing performed in GEE utilizes the Analysis Ready Data Preparation Toolkit for terrain correction, border noise removal, and decibel conversion. To find burn area, an approach outlined by Ajadi et al. (2016) will be utilized and has been provided for use by the ASF for the Python processing portion of the methodology (See Figure 3).

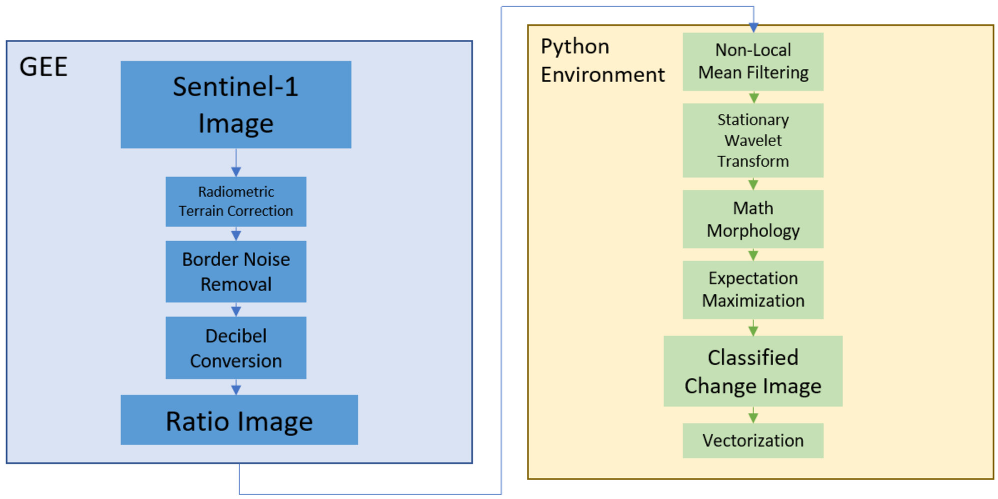

Figure 3. Flowchart of data processing. The Analysis Ready Data Preparation toolkit performs the terrain correction, border noise removal, and decibel conversion in GEE.

The first step is to query the study area for the specific images for both the ascending and descending orbit passes and process the data through the GEE application, Analysis Ready Data Preparation toolkit. Using these set of tools, the selected Sentinel-1 images receive some radiometric terrain correction with some of the distortion effects from the terrain removed. This is particularly necessary for the Woods Creek Fire and the French Fire which both occurred in mountainous terrain. While radiometric terrain correction allows for images to be compared outside of the same relative orbit, it is necessary in this case to compare the imagery with similar geometry along the side of the mountain to minimize the impact of slope aspect.

The radiometric terrain correction performed is an angular based correction using a digital elevation model (DEM) in GEE. This makes use of the Sentinel-1 incidence angle that is also present with the Sentinel-1 dataset. It is recommended that a DEM in the same resolution as the image data is used to perform a correction. The 3D Elevation Program (3DEP) DEM from USGS at a 10-meter resolution which was derived from lidar was used for terrain correction. This increases the fidelity of the terrain correction compared to the 30-meter SRTM DEM. This backscatter correction is based off the terrain and SAR incidence angle (Vollrath et al. 2020). More complex forms of radiometric terrain corrections are not used because of the limited nature of the GRD imagery data within GEE (Vollrath et al. 2020). Other methods to perform terrain correction use the SLC data which includes the SAR phase information as well as methods which use a simulated SAR image from a DEM to correct the radar image (Hoekman and Reiche 2015, Small 2011, Loew and Mauser 2007).

The next step is to remove noise prone areas along the border of the Sentinel-1 images using the toolkit. This removal is based on an incidence angle mask in order to minimize noise based on non-optimal incidence angles along the edge of an image (Hird et al. 2017). The images are then converted from the original linear power values to decibel (10*log10(x)) format which helps normalize the image to make brighter pixels more distinguishable from darker pixels. From there, a ratio image is created in GEE between the reference image and the comparison image of image pairs and will be ready for the change detection. Since the image has been logarithmically scaled it is important to note that the difference of these two images is a logarithmic ratio. Here, the ratio images are downloaded for processing in a Python environment where they are run through a modified version of the script by Ajadi et al. (2016).

Following preprocessing, the process described by Ajadi et al. (2016) is to perform non-local means filtering on the image. As described by Ajadi et al. (2016), non-local means filtering allows for radar speckle—which is caused by interference during the acquisition of an image— in the images to be filtered uniformly across the scene with minimal loss of detail. This is a departure from the process described by the original authors since now the ratio image is first created within GEE before processing using non-local means filtering. The original methodology used images processed first with non-local means filtering before the ratio image was made. The reason for this change is to make use of GEE's image processing and georeferencing so that these additional steps would not need to be performed in Python.

Next is to apply a two-dimensional stationary wavelet transform. The two-dimensional stationary wavelet transform allows for a multiscale approach to look at areas of change by filtering most of the prevailing parts of the image at various decomposition levels. A lower decomposition level produces an image that is closer to the original input scale and uses less computational power though has higher levels of noise. Higher decomposition levels resolve changes in an image by reconstructing the image so the prevailing geometry is preserved without the high noise components but uses more computational power. This is followed by performing math morphology to help pull out bright or darkened areas from the ratio image through a process of opening and closing regions. This process helps to further reduce noise while preserving details along the edges of regions.

Expectation maximization is utilized to help calculate the change classes. As stated by Ajadi et al. (2016), this assumes that the SAR imagery in decibels has characteristics of a Gaussian curve. This finds the local maximums on the image histogram which can then be used to establish class thresholds. The number of classes chosen is incrementally approached though the use of the sum of square error (SSE) to check against the image. An overview of these steps performed on an image can be seen in Figure 4.

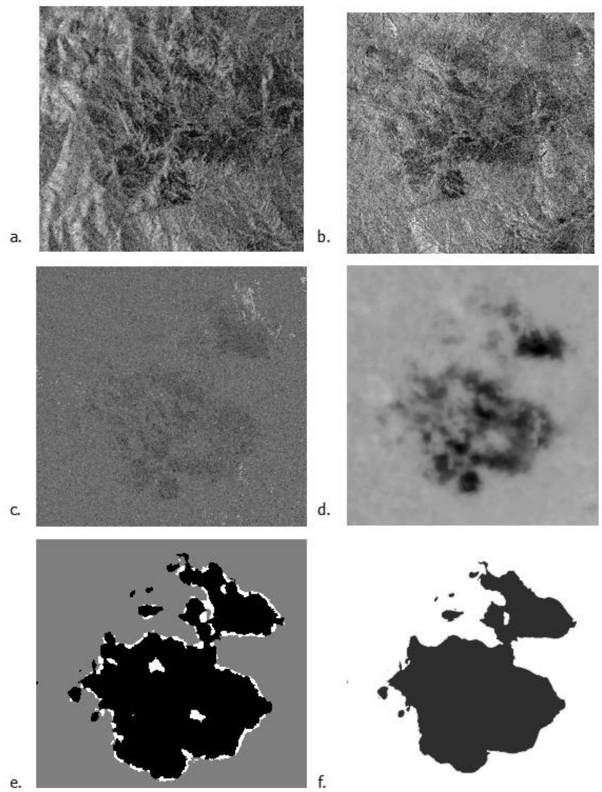

Figure 4. Overview of processing on an image. This example uses the ascending August 28 Sentinel-1 Image in the VH polarity for the French Fire, CA a.) The original GRD SAR image range: -27.5dB to-2.4dB; b.) Slope corrected SAR image range: -26.7dB to -2.9dB; c.) Ratio image range -30.5dB to 41.2dB; d.) Ratio image after wavelet filtering and math morphology range: -115.4dB to 65.1 dB; e.) Expectation Maximization creates two change classes and one class of no change; f.) Vectorized and filled areas of change.

The parameters that were used at first were the suggested parameters of a 20 by 20 pixel structure element in the math morphology step, six decompositions for the stationary wavelet transform and up to three classes during the expectation maximization step. This was later changed to 30 by 30 pixel structure element for the math morphology, four decompositions in the stationary wavelet transform and up to ten classes for expectation maximation for all the images of the Woods Creek Fire. The descending orbit of the French fire uses recommended parameters while the ascending orbit used a smaller structure element of 10 by 10 pixels for math morphology.

After these steps, the resulting classified image is converted to change and no change areas. These areas are then vectorized and compared to Sentinel-2 dNBR and the MODIS Burn Area images to examine the accuracy of the Sentinel-1 burn area product. This step compares the Sentinel-2 dNBR to both the ascending and descending orbits passes of the SAR burn area due to the potential terrain effects despite the correction efforts. While radiometric terrain correction mitigates effects from terrain in the collected images, there is still potential for missed data or readings by the sensor due to radar shadow effects and void areas from the terrain.

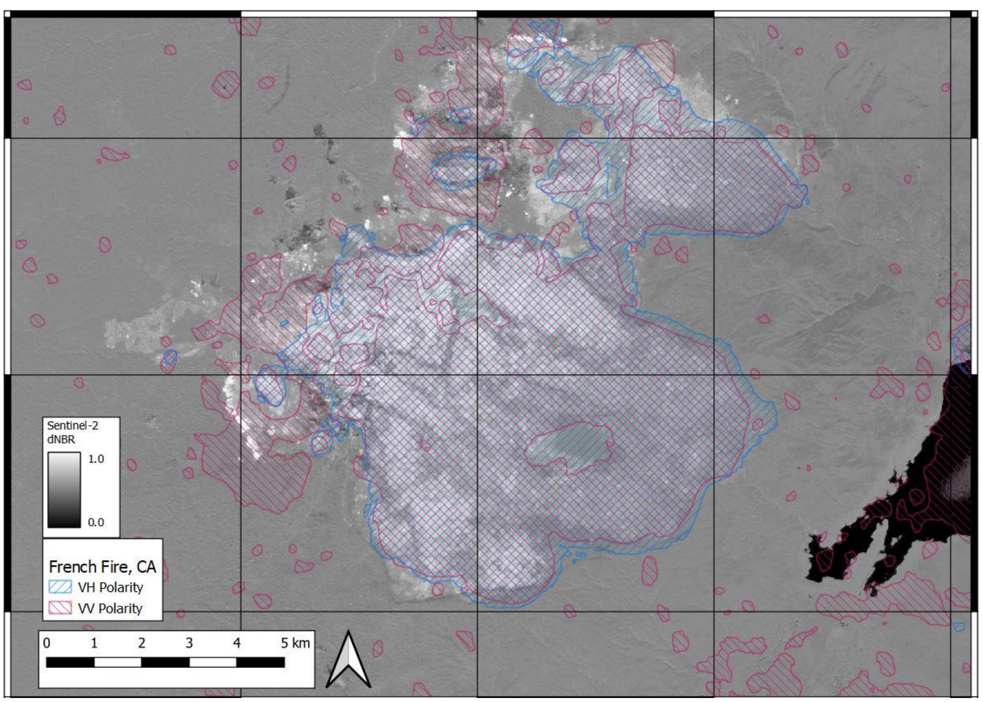

Figure 5. Overview of the French Fire, CA with the VV and VH polarity SAR burn areas from August 28, 2021 over the dNBR image from August 25, 2021. Brighter areas indicate more severe burning.

The optical imagery that is compared will be from a similar time period as the ratio images looked at. An example of this can be seen in the NBR image with SAR burn areas in Figure 5, The dNBR was categorized into four different threshold classes: low, medium low, medium high, and high (See Table 4). The Sentinel-2 bands used were band 8 and band 12 which correspond to the NIR and SWIR wavelengths respectively. In the same light, the MODIS burn areas will be compared against the SAR imagery though is of a much lower resolution at about 500 meters per pixel compared to the Sentinel-2's 20-meter pixel.

Table 4. The Sentinel-2 dNBR burn severity thresholds used for comparison against the SAR burn area.

Burn Severity	dNBR
Low	0.10-0.27
Moderate Low	0.27-0.44
Moderate High	0.44-0.66
High	>0.66

IV. RESULTS

An accuracy assessment for the producer's accuracy, user's accuracy, overall accuracy and Cohen's kappa coefficient was performed on each image for both locations comparison of the Sentinel-1 SAR results to the various levels of Sentinel-2 dNBR as well as to the MODIS Burn Area Product. Confusion matrices for the Sentinel-1 SAR burn area against both the Sentinel-2 dNBR and MODIS Burn Area can be found in the Appendix. The producer, user, and overall accuracy were selected as metrics in order to evaluate how well the SAR burn area method is compared to optical burn area calculations. Cohen's kappa was selected as an additional metric in order to compare these methods directly and to describe how well they agree with one another. One thousand sample points were generated in each of the two areas of interest within a bounding box. Land cover type was not considered for the burn area since the desire is to evaluate the methodology on unmasked SAR imagery.

Sentinel-2 images that were used were selected to be temporally coincidental to the Sentinel-1 images as much as possible. The main limiting factor to this was image availability due to cloud cover over the study area therefore cloud covered images were kept to a minimum for the dates that were looked at. These images were manually filtered to ensure the study area was not obscured by clouds. This is the case for both the pre-fire image as well as the fire event image. Four burn thresholds for dNBR analysis—low, moderate-low, moderate-high, and high burn ratio—were used and each compared to the SAR data.

The MODIS selected Burn Area data, like the Sentinel-2 data, was as close to the imaging date of the Sentinel-1 images as possible. The maximum extent burn area was used for the September comparisons for both the Woods Creek Fire and the French Fire.

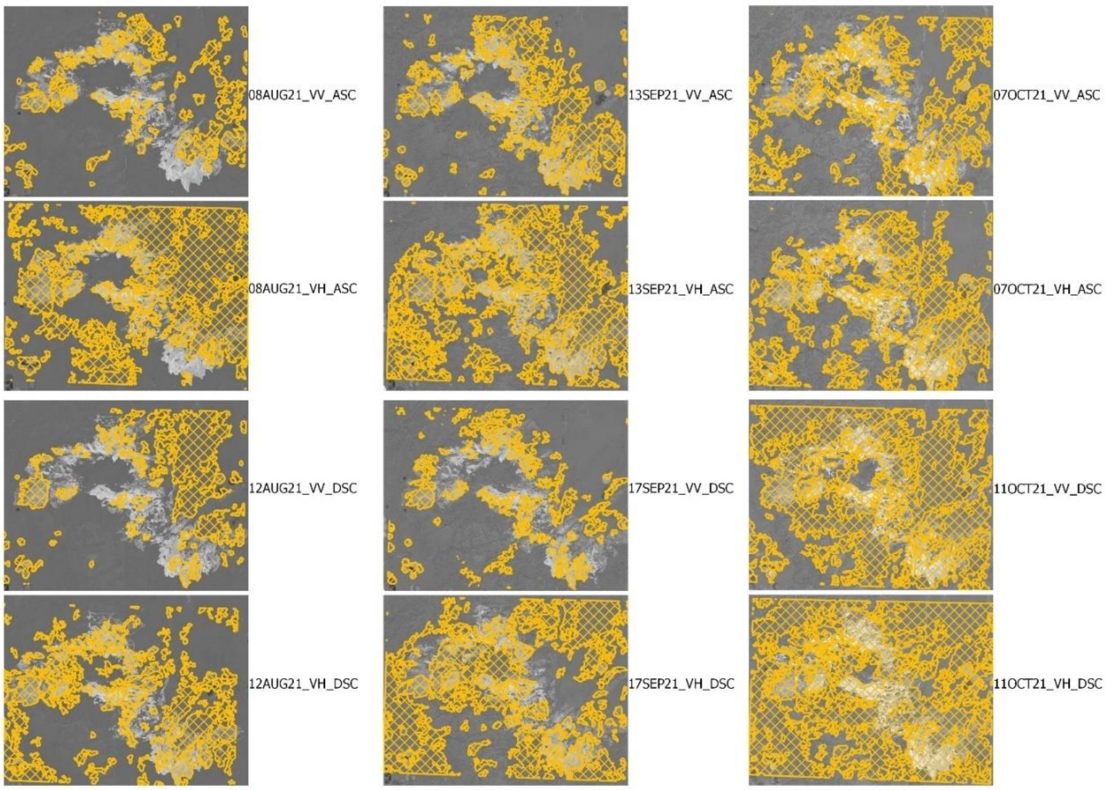

Figure 6. Burn areas identified by the SAR for the Woods Creek Fire. In each plot, the label gives the date (ex., 08AUG21), polarity (VV or VH), and ascending (ASC) or descending (DSC). The identified SAR burned pixels are in yellow hatch marks overlaid on the Sentinel-2 dNBR image (gray scale) for the corresponding date.

The overall accuracy of the Woods Creek Fire utilizing this method shows that there was notable inconsistency over the area that was looked at for the chosen dates. The SAR data that had the best results were the VV polarity in the ascending pass while the least favorable results were those of the VH polarity particularly in the descending orbit.

The VV polarity SAR data had high accuracies against the moderate high and high dNBR data in the ascending pass. The descending pass VV SAR data was less consistent over the time period looked at with October having the lowest accuracy of all the co-polarized data for Montana. This can be particularly observed in Figure 6 when looking at the burn area maps for the fire. VV burn area for most of the ascending and descending data follows burn area closely to the Sentinel-2 dNBR than the VH data for the Woods Creek Fire. However, the August SAR burn area had the highest accuracy at the Woods Creek Fire at 84.4% when compared to the high dNBR for the month. The overall accuracy of the VH SAR burn area shows a low overall accuracy across the various levels of dNBR as well as MODIS which can be seen in Figure 7. The October descending VH SAR burn area had the lowest overall accuracy as well.

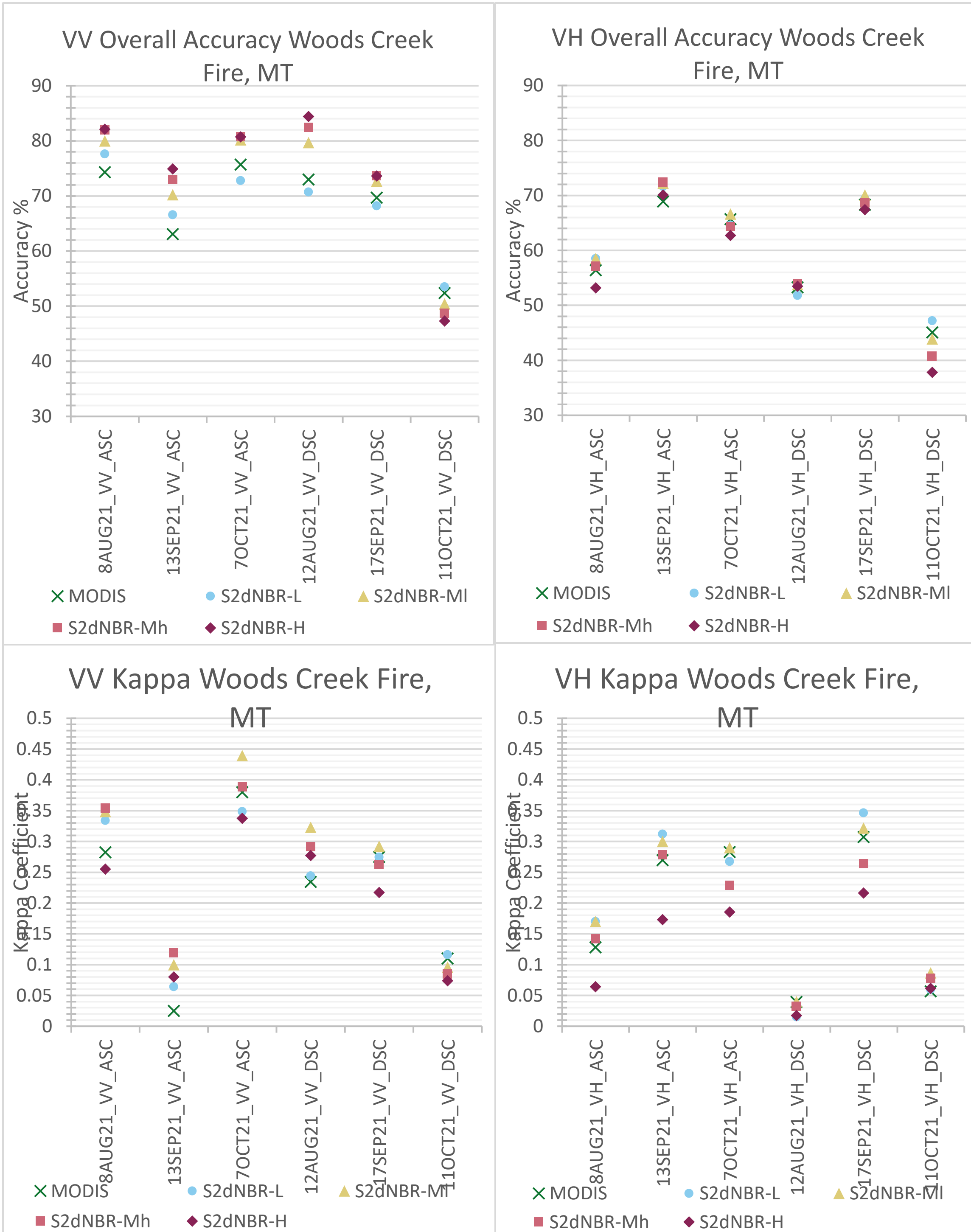

Figure 7. Overall accuracy and kappa coefficient values against the MODIS and Sentinel-2 burned area identification for the MT fire. The notations for the SAR cases are the same as those used in Figure 6. Four thresholds (Low [L], Moderate Low [Ml], Moderate High (Mh), and High [H]) for dNBR burn severity with Sentinel-2 (S2) are treated separately.

The Cohen's kappa for the Woods Creek Fire shows that the results were very random with low kappa coefficients which explains the spotty results when looking at the results displayed spatially. The possible reasons for this are brought up in the discussion. The moderate-low Sentinel-2 dNBR had the least amount of randomness across orbit and polarity (See Figure 7). MODIS in comparison consistently takes the middle ground when compared with the NBR data. There was not much of a pattern in the amount of randomness when splitting the data up between the polarities.

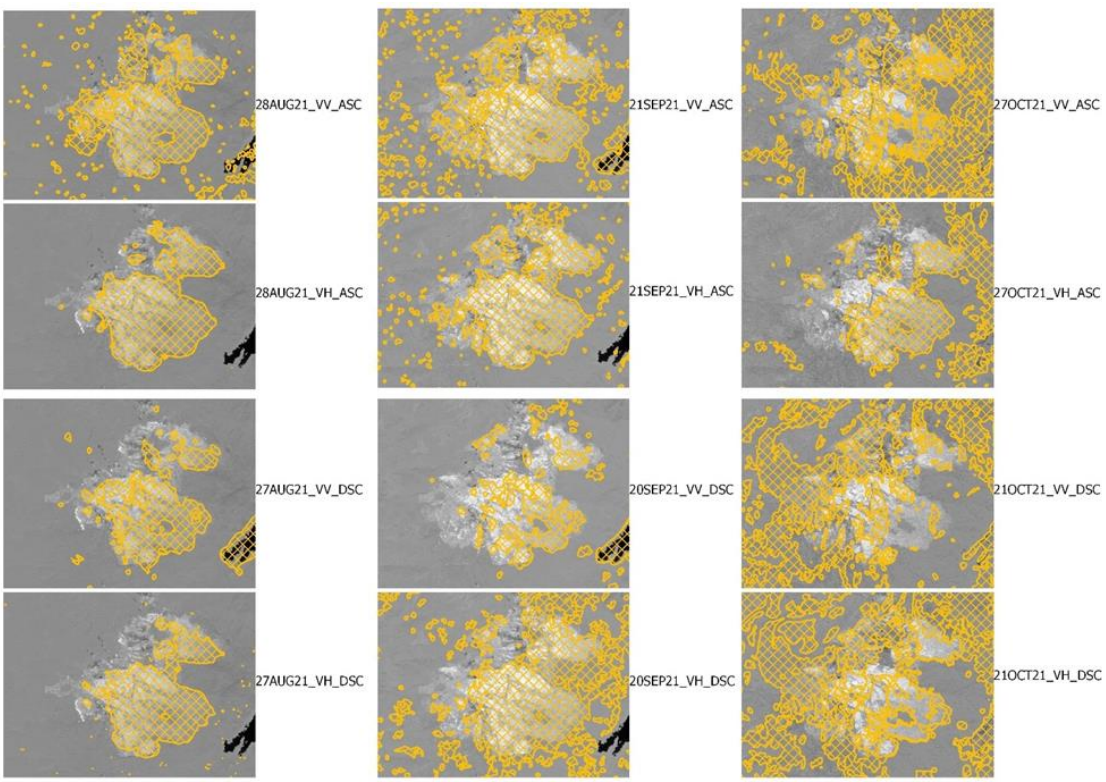

Figure 8. Burn areas identified by the SAR for the French Fire. In each plot, the label gives the date (ex., 28AUG21), polarity (VV or VH), and ascending (ASC) or descending (DSC). The identified SAR burned pixels are in yellow hatch marks overlaid on the Sentinel-2 dNBR image (gray scale) for the corresponding date.

The overall accuracy of the French Fire is much more consistent between the polarities. Figure 8 shows that the ascending orbit gave the best results with stronger results from the VH polarity as opposed to the VV polarity. Overall, the ascending orbit had a higher accuracy for both polarities than the descending orbit. The comparison of SAR burn area against the moderate-low Sentinel-2 dNBR was the most consistent in both polarities for the ascending orbit direction with over 80% accuracy as seen in Figure 9. When compared against the other dNBR levels in the ascending orbit, the accuracy of the SAR data was much more varied. SAR burn area comparison with the MODIS data gave good results, though not as strong as some of the other dNBR levels likely to the limiting factor of resolution on this smaller fire. The descending orbit burn area results were not as strong as the ascending orbit with much lower overall accuracies for the September and October VV SAR burn area and lower accuracies throughout with the VH polarity. Overall accuracy on the same time period in the VH data was much closer between the various dNBR levels than the VV SAR burn areas. These results for the French Fire in Figure 9 show there is agreeance between the SAR data and the optical data for both Sentinel-2 dNBR and the MODIS burn areas. Overall accuracy was as high as 87.4% in the VH polarity when compared to the low Sentinel-2 NBR on using the SAR image from August 28, 2021. Likewise, SAR comparison to the MODIS on this date was found to be an 85% overall accuracy.

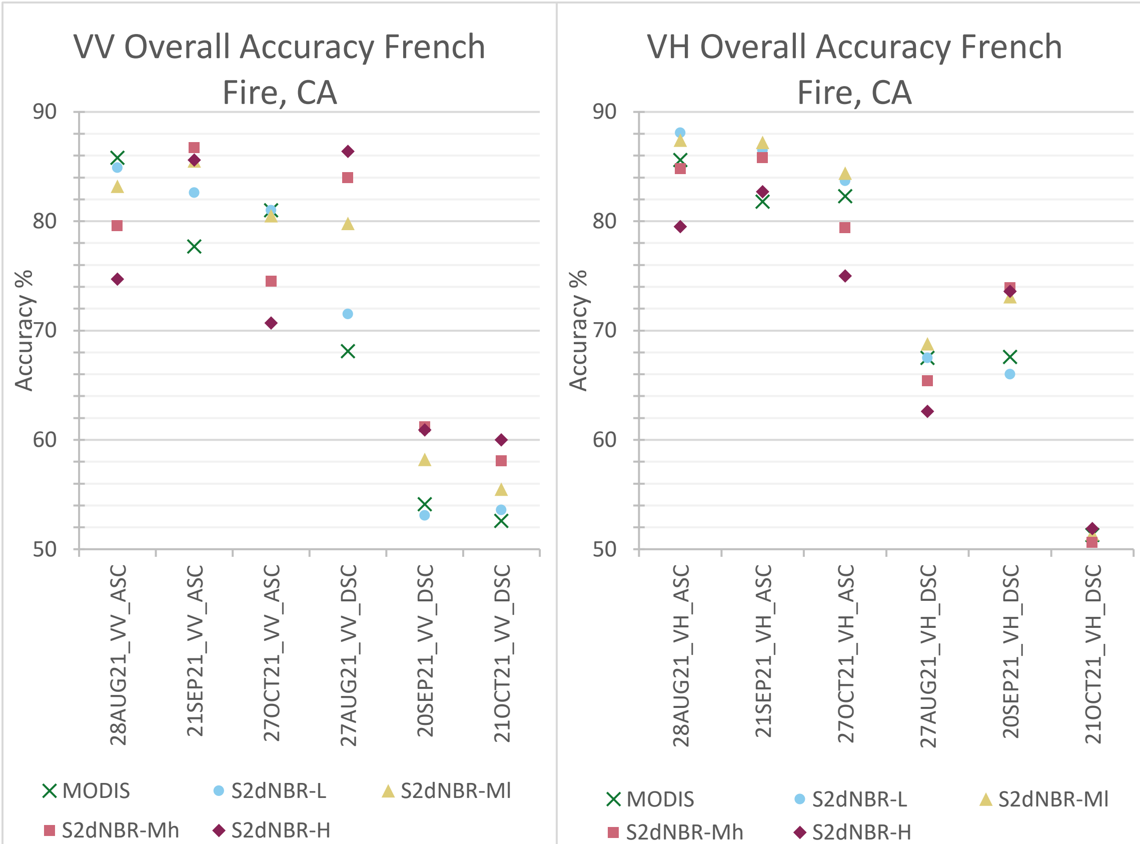

Figure 9. Overall accuracy values against the MODIS and Sentinel-2 burned area identification for the CA fire. The notations for the SAR cases are the same as those used in Figure 8. Four thresholds (Low [L], Moderate Low [Ml], Moderate High (Mh), and High [H]) for dNBR burn severity with Sentinel-2 (S2) are treated separately.

Figure 10 shows kappa Coefficient for the French Fire with more randomness in the descending orbits. Cohen’s kappa for the French Fire shows that the ascending orbit SAR burn area was not random when compared against dNBR resulting in high kappa coefficients. The results of the low Sentinel-2 dNBR had the least random results followed by the moderate-low, the moderate-high, then high dNBR levels. The VH polarity had slightly lower randomness—or higher kappa values—compared to the VV polarity. SAR comparison with the MODIS burn areas also showed low randomness compared comparable to that of the low and moderate-low Sentinel-2 dNBR. Comparing this orbit to the descending orbit shows that the descending orbit exhibited much more randomness in the results with the October SAR burn area being the most random of all the data compared against Sentinel-2 and MODIS imagery.

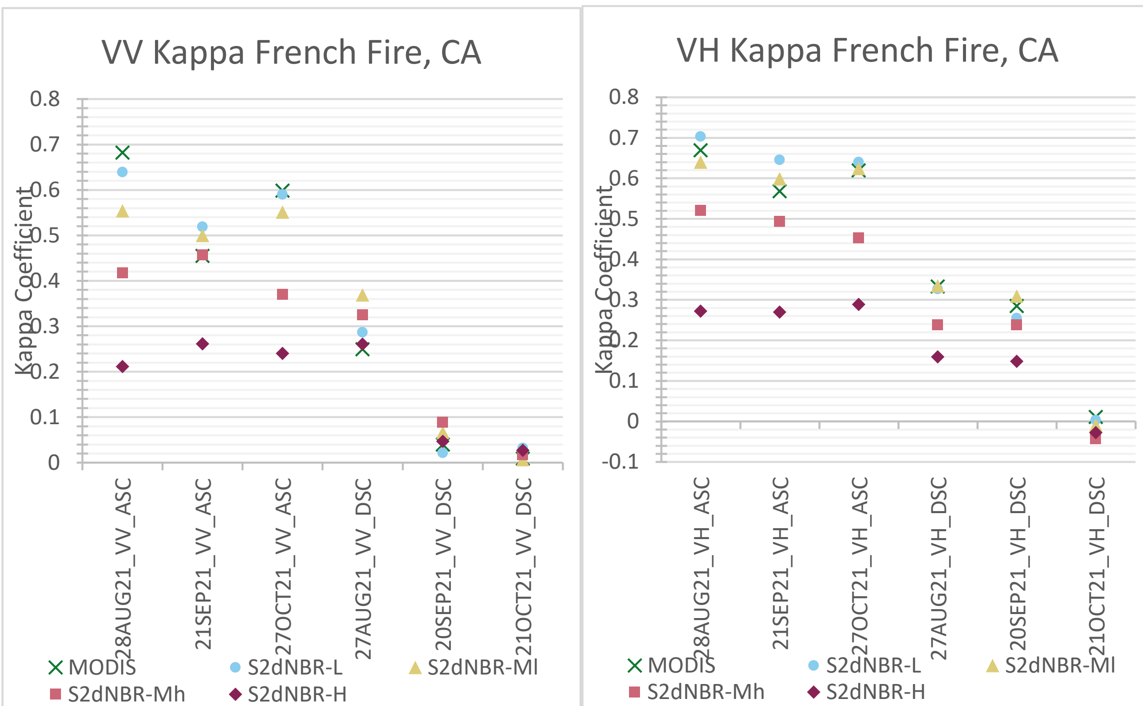

Figure 11. kappa coefficient against the MODIS and Sentinel-2 burned area identification for the CA fire. The notations for the SAR cases are the same as those used in Figure 8. Four thresholds (Low [L], Moderate Low [Ml], Moderate High (Mh), and High [H]) for dNBR burn severity with Sentinel-2 (S2) are treated separately.

V. DISCUSSION

Dialing in the parameters of the math morphology and expectation maximization to get accurate change detection proved to be difficult at first with results showing very minimal change in the SAR imagery as opposed to the optical imagery. At first, the results did not fit well at the Woods Creek fire for any of the dates using the recommended parameters. The parameters were changed from the recommended in order to get a better representation of change occurring at the site of the fire. The parameters that worked best for the Woods Creek Fire used a math morphology structure element of 30 by 30 pixels—where dilation and erosion will use 30 pixel squares, in addition to increasing the number of change classes to ten during expectation maximization. This is to help take into account other activities occurring in the scene that may be influencing change such as agriculture, changes in the nearby lake, and variances in extreme terrain. These parameters were used for both the ascending and the descending passes for this fire.

For the French Fire, the recommended values were used for the descending orbit. The recommended values used a 20 by 20 pixel structure element for the math morphology step where the dilation and erosion use a 20 pixel square, six decompositions for the stationary wavelet transform, and three classes for expectation maximization. Six decompositions were used since this was a smaller fire and was not as computationally intensive due to less area being processed. The ascending orbit was changed slightly using a 10 by 10 pixel structure element in the math morphology step in order to help reduce some added noise from a larger structure element.

Results show that the SAR burn area for the Woods Creek Fire in Montana had a lot of randomness to it. While visually it is possible to see where a burn area might be, there are larger areas which were not included in the optical burn area. This is likely due to a few factors in the data itself and the processing of the data. As the fire was mostly on the western part of the mountain, the ascending pass was more advantageous picking up the leftover burn scar from the fire but had a hard time on the eastern side of the mountain. Additionally, the method of terrain correction was likely not good enough for the amount terrain present for this fire due to it spanning over both the eastern and western slopes of the mountain. The terrain flattening that was used did not rely on any of the orbit data present for Sentinel-1 since the data was processed from data within the GEE catalog which is absent of the precise orbit data that are published by ESA.

Despite the problems, the VV polarity across both orbit directions was consistently better than the VH polarity. This is most likely due to the coniferous forests which are present in this area of the United States. While the VH polarity had better results when being compared to the Sentinel-2 dNBR on only one occasion from the ascending orbit on September 13, 2021.

The SAR comparison to the Sentinel-2 and the MODIS imagery of the French Fire had comparable results to each other. The results turned out well despite using the terrain correction algorithm based solely on incidence angle and slope aspect. What was expected and seen in the Sentinel-2 dNBR comparisons was that the SAR burn areas were more similar to the lower categories of burn severity than the high categories of burn severity, with the highest levels of accuracy alternating between the low or the moderate low burn severity categories. This may vary in other scenarios absent any quad-polarity data since SAR is dependent on collection geometry.

In evaluating both the Montana and the California area of interests, the SAR burn area seems to follow closely that of the moderate-low Sentinel-2 dNBR using this methodology as it currently is and also follows the burn areas of MODIS decently as well.

VI. CONCLUSION

The goal of this research is to search for methods with SAR imagery to detect burn area and monitor change quickly. In one case, the burned area in SAR is similar to the area on optical imagery with the French Fire in California. This research partially showed how well burned area can be detected in an area with a moderate amount of terrain effects despite minimal terrain correction with one of the two locations being a good example. Burn area using SAR as a method for detection is viable in areas where the amount of terrain is fairly moderate and the geometries of the SAR collection work out. Terrain correction method impacts how successful SAR satellites are utilized for wildfires especially in the North American West where wildfire commonly occurs. This research will also support the further utilization of cloud based remote sensing analysis in which this method is performed on a platform such as GEE. This research additionally sets up opportunities for further research to compare SAR imagery collected from different orbital directions.

One of the limitations of this research is the type of terrain correction under the scope of GEE with the available data. An alternative data source of radiometrically terrain corrected SAR imagery could have been acquired through the ASF's Hybrid Pluggable Processing Pipeline (HyP3). This could potentially be topic for future research. Some of the other difficulties of this methodology include the need to fine tune the parameters to make sure that it is not overrepresenting or underrepresenting the change present on the ground. This may also be future research area for the comparisons of terrain correction methods.

A limitation on the data itself is that the Sentinel-1 SAR imagery is collected at a different time and periodicity from the Sentinel-2 multispectral imagery. Wildfire is a dynamic event and thus a one-to-one comparison between the data is not able to be made. Additionally, the SAR imagery is differentiating a change in structure between two time periods while the optical imagery is differentiating a change in chemistry between two time periods. Precipitation could have an impact on the SAR backscatter values and could impact actual change between the time period. An ascending pass may have different results from a descending pass in areas of high terrain or the cross-polarity change could have a different result from the co-polarity change. Clearly understanding the effect of orbit direction or polarity would also be useful when designing or planning SAR systems in support of wildfires or for forest management.

Additionally, while this project looked at Sentinel-1 SAR imagery sampling dates over a longer period of time, another research area could have been how well this algorithm can perform against successive images over the study area over a shorter time period early on in the lifecycle of a wildfire. Land cover could be looked at based upon how sensitive C-Band SAR is to certain vegetation types and using various land cover datasets in conjunction with this methodology as well.

Understanding and utilizing SAR imagery for wild fire has the potential for it to being used in areas in which normal optical imagery will not be able to image due to clouds, smoke or to be able to get a burn area for areas in which airborne flying over may be difficult due to it being a very remote area or in a denied airspace.

APPENDIX

Appendix: confusion matrices; user's, producer's and overall accuracies for all cases.

Woods Creek Fire, MONTANA

August Ascending

VV	Reference Sentinel-2 Low dNBR			
SAR – Sentinel-1	**No burn**	**Burn**	**SAR total**	**User's %**
No burn	*680*	*171*	*851*	**79.90599**
Burn	*53*	*96*	*149*	**64.42953**
Ref. total	*733*	*267*	*1000*	
Producer's %	**92.7694407**	**35.95506**	**Overall %**	**77.6**

VH	Reference Sentinel-2 Low dNBR			
SAR – Sentinel-1	**No burn**	**Burn**	**SAR total**	**User's %**
No burn	409	*91*	*500*	**81.8**
Burn	*324*	*176*	*500*	**35.2**
Ref. total	*733*	*267*	*1000*	
Producer's %	**55.79809**	**65.9176**	**Overall %**	**58.5**

VV	Reference Sentinel-2 Moderate Low dNBR			
SAR – Sentinel-1	**No burn**	**Burn**	**SAR total**	**User's %**
No burn	*713*	*138*	*851*	**83.78378**
Burn	*62*	*87*	*149*	**58.38926**
Ref. total	*775*	*225*	*1000*	
Producer's %	**92**	**38.66667**	**Overall %**	**80**

VH	Reference Sentinel-2 Moderate Low dNBR			
SAR – Sentinel-1	**No burn**	**Burn**	**SAR total**	**User's %**
No burn	430	*70*	*500*	**86**
Burn	*345*	*155*	*500*	**31**
Ref. total	*775*	*225*	*1000*	
Producer's %	**55.483871**	**68.88889**	**Overall %**	**58.5**

VV	Reference Sentinel-2 Moderate High dNBR			
SAR – Sentinel-1	**No burn**	**Burn**	**SAR total**	**User's %**
No burn	*743*	*108*	*851*	**87.30905**
Burn	*72*	*77*	*149*	**51.67785**
Ref. total	*815*	*185*	*1000*	
Producer's %	**91.1656442**	**41.62162**	**Overall %**	**82**

VH	Reference Sentinel-2 Moderate High dNBR			
SAR – Sentinel-1	**No burn**	**Burn**	**SAR total**	**User's %**
No burn	443	*57*	*500*	**88.6**
Burn	*372*	*128*	*500*	**25.6**
Ref. total	*815*	*185*	*1000*	
Producer's %	**54.3558282**	**69.18919**	**Overall %**	**57.1**

VV	Reference Sentinel-2 High dNBR			
SAR – Sentinel-1	**No burn**	**Burn**	**SAR total**	**User's %**
No burn	*771*	*80*	*851*	**90.59929**
Burn	*99*	*50*	*149*	**33.55705**
Ref. total	*870*	*130*	*1000*	
Producer's %	**88.6206897**	**38.46154**	**Overall %**	**82.1**

VH	Reference Sentinel-2 High dNBR			
SAR – Sentinel-1	**No burn**	**Burn**	**SAR total**	**User's %**
No burn	451	*49*	*500*	**90.2**
Burn	*419*	*81*	*500*	**16.2**
Ref. total	*870*	*130*	*1000*	
Producer's %	**51.8390805**	**62.30769**	**Overall %**	**53.2**

VV	Reference MODIS Burn				VH	Reference MODIS Burn			
SAR – Sentinel-1	**No burn**	**Burn**	**SAR total**	**User's %**	**SAR – Sentinel-1**	**No burn**	**Burn**	**SAR total**	**User's %**
No burn	*648*	*203*	*851*	**76.14571**	No burn	383	*117*	*500*	**76.6**
Burn	*54*	*95*	*149*	**63.75839**	Burn	*319*	*181*	*500*	**36.2**
Ref. total	*702*	*298*	*1000*		Ref. total	*702*	*298*	*1000*	
Producer's %	**92.3076923**	**31.87919**	**Overall %**	**74.3**	**Producer's %**	**54.5584046**	**60.73826**	**Overall %**	**56.4**

August Descending

VV	Reference Sentinel-2 Low dNBR				VH	Reference Sentinel-2 Low dNBR			
SAR – Sentinel-1	**No burn**	**Burn**	**SAR total**	**User's %**	**SAR – Sentinel-1**	**No burn**	**Burn**	**SAR total**	**User's %**
No burn	*603*	*204*	*807*	**74.72119**	No burn	568	*119*	*687*	**82.67831**
Burn	*130*	*63*	*193*	**32.64249**	Burn	*165*	*148*	*313*	**47.28435**
Ref. total	*733*	*267*	*1000*		Ref. total	*733*	*267*	*1000*	
Producer's %	**82.2646658**	**23.59551**	**Overall %**	**66.6**	**Producer's %**	**77.4897681**	**55.43071**	**Overall %**	**71.6**

VV	Reference Sentinel-2 Moderate Low dNBR				VH	Reference Sentinel-2 Moderate Low dNBR			
SAR – Sentinel-1	**No burn**	**Burn**	**SAR total**	**User's %**	**SAR – Sentinel-1**	**No burn**	**Burn**	**SAR total**	**User's %**
No burn	*642*	*165*	*807*	**79.5539**	No burn	592	*95*	*687*	**86.17176**
Burn	*133*	*60*	*193*	**31.08808**	Burn	*183*	*130*	*313*	**41.53355**
Ref. total	*775*	*225*	*1000*		Ref. total	*775*	*225*	*1000*	
Producer's %	**82.8387097**	**26.66667**	**Overall %**	**70.2**	**Producer's %**	**76.3870968**	**57.77778**	**Overall %**	**72.2**

VV	Reference Sentinel-2 Moderate High dNBR			
SAR – Sentinel-1	**No burn**	**Burn**	**SAR total**	**User's %**
No burn	*676*	*131*	*807*	**83.76704**
Burn	*139*	*54*	*193*	**27.97927**
Ref. total	*815*	*185*	*1000*	
Producer's %	**82.9447853**	**29.18919**	**Overall %**	**73**

VH	Reference Sentinel-2 Moderate High dNBR			
SAR – Sentinel-1	**No burn**	**Burn**	**SAR total**	**User's %**
No burn	613	*74*	*687*	**89.22853**
Burn	*202*	*111*	*313*	**35.46326**
Ref. total	*815*	*185*	*1000*	
Producer's %	**75.2147239**	**60**	**Overall %**	**72.4**

VV	Reference Sentinel-2 High dNBR			
SAR – Sentinel-1	**No burn**	**Burn**	**SAR total**	**User's %**
No burn	*713*	*94*	*807*	**88.35192**
Burn	*157*	*36*	*193*	**18.65285**
Ref. total	*870*	*130*	*1000*	
Producer's %	**81.954023**	**27.69231**	**Overall %**	**74.9**

VH	Reference Sentinel-2 High dNBR			
SAR – Sentinel-1	**No burn**	**Burn**	**SAR total**	**User's %**
No burn	629	*58*	*687*	**91.5575**
Burn	*241*	*72*	*313*	**23.00319**
Ref. total	*870*	*130*	*1000*	
Producer's %	**72.2988506**	**55.38462**	**Overall %**	**70.1**

VV	Reference MODIS Burn			
SAR – Sentinel-1	**No burn**	**Burn**	**SAR total**	**User's %**
No burn	568	239	*807*	**70.38414**
Burn	130	63	*193*	**32.64249**
Ref. total	*698*	*302*	*1000*	
Producer's %	**81.3753582**	**20.86093**	**Overall %**	**63.1**

VH	Reference MODIS Burn			
SAR – Sentinel-1	**No burn**	**Burn**	**SAR total**	**User's %**
No burn	537	150	*687*	**78.16594**
Burn	161	152	*313*	**48.5623**
Ref. total	*698*	*302*	*1000*	
Producer's %	**76.9340974**	**50.33113**	**Overall %**	**68.9**

September Ascending

VV	Reference Sentinel-2 Low dNBR			
SAR – Sentinel-1	**No burn**	**Burn**	**SAR total**	**User's %**
No burn	*576*	*197*	*773*	**74.51488**
Burn	*75*	*152*	*227*	**66.96035**
Ref. total	*651*	*349*	*1000*	
Producer's %	**88.4792627**	**43.55301**	**Overall %**	**72.8**

VH	Reference Sentinel-2 Low dNBR			
SAR – Sentinel-1	**No burn**	**Burn**	**SAR total**	**User's %**
No burn	426	*129*	*555*	**76.75676**
Burn	*225*	*220*	*445*	**49.4382**
Ref. total	*651*	*349*	*1000*	
Producer's %	**65.437788**	**63.03725**	**Overall %**	**64.6**

VV	Reference Sentinel-2 Moderate Low dNBR			
SAR – Sentinel-1	**No burn**	**Burn**	**SAR total**	**User's %**
No burn	*672*	*101*	*773*	**86.93402**
Burn	*97*	*130*	*227*	**57.26872**
Ref. total	*769*	*231*	*1000*	
Producer's %	**87.3862159**	**56.27706**	**Overall %**	**80.2**

VH	Reference Sentinel-2 Moderate Low dNBR			
SAR – Sentinel-1	**No burn**	**Burn**	**SAR total**	**User's %**
No burn	495	*60*	*555*	**89.18919**
Burn	*274*	*171*	*445*	**38.42697**
Ref. total	*769*	*231*	*1000*	
Producer's %	**64.3693108**	**74.02597**	**Overall %**	**66.6**

VV	Reference Sentinel-2 Moderate High dNBR			
SAR – Sentinel-1	**No burn**	**Burn**	**SAR total**	**User's %**
No burn	*709*	*64*	*773*	**91.72057**
Burn	*129*	*98*	*227*	**43.17181**
Ref. total	*838*	*162*	*1000*	
Producer's %	**84.6062053**	**60.49383**	**Overall %**	**80.7**

VH	Reference Sentinel-2 Moderate High dNBR			
SAR – Sentinel-1	**No burn**	**Burn**	**SAR total**	**User's %**
No burn	518	*37*	*555*	**93.33333**
Burn	*320*	*125*	*445*	**28.08989**
Ref. total	*838*	*162*	*1000*	
Producer's %	**61.8138425**	**77.16049**	**Overall %**	**64.3**

VV	Reference Sentinel-2 High dNBR			
SAR – Sentinel-1	**No burn**	**Burn**	**SAR total**	**User's %**
No burn	*731*	*42*	*773*	**94.56662**
Burn	*151*	*76*	*227*	**33.48018**
Ref. total	*882*	*118*	*1000*	
Producer's %	**82.8798186**	**64.40678**	**Overall %**	**80.7**

VH	Reference Sentinel-2 High dNBR			
SAR – Sentinel-1	**No burn**	**Burn**	**SAR total**	**User's %**
No burn	532	*23*	*555*	**95.85586**
Burn	*350*	*95*	*445*	**21.34831**
Ref. total	*882*	*118*	*1000*	
Producer's %	**60.3174603**	**80.50847**	**Overall %**	**62.7**

VV	Reference MODIS Burn			
SAR – Sentinel-1	**No burn**	**Burn**	**SAR total**	**User's %**
No burn	*614*	*159*	*773*	**79.43079**
Burn	*84*	*143*	*227*	**62.99559**
Ref. total	*698*	*302*	*1000*	
Producer's %	**87.965616**	**47.35099**	**Overall %**	**75.7**

VH	Reference MODIS Burn			
SAR – Sentinel-1	**No burn**	**Burn**	**SAR total**	**User's %**
No burn	455	*100*	*555*	**81.98198**
Burn	*243*	*202*	*445*	**45.39326**
Ref. total	*698*	*302*	*1000*	
Producer's %	**65.1862464**	**66.88742**	**Overall %**	**65.7**

September Descending

VV	Reference Sentinel-2 Low dNBR			
SAR – Sentinel-1	**No burn**	**Burn**	**SAR total**	**User's %**
No burn	*615*	*257*	*872*	**70.52752**
Burn	*36*	*92*	*128*	**71.875**
Ref. total	*651*	*349*	*1000*	
Producer's %	**94.4700461**	**26.36103**	**Overall %**	**70.7**

VH	Reference Sentinel-2 Low dNBR			
SAR – Sentinel-1	**No burn**	**Burn**	**SAR total**	**User's %**
No burn	352	*183*	*535*	**65.79439**
Burn	*299*	*166*	*465*	**35.69892**
Ref. total	*651*	*349*	*1000*	
Producer's %	**54.0706605**	**47.56447**	**Overall %**	**51.8**

VV	Reference Sentinel-2 Moderate Low dNBR			
SAR – Sentinel-1	**No burn**	**Burn**	**SAR total**	**User's %**
No burn	*719*	*153*	*872*	**82.45413**
Burn	*50*	*78*	*128*	**60.9375**
Ref. total	*769*	*231*	*1000*	
Producer's %	**93.4980494**	**33.76623**	**Overall %**	**79.7**

VH	Reference Sentinel-2 Moderate Low dNBR			
SAR – Sentinel-1	**No burn**	**Burn**	**SAR total**	**User's %**
No burn	421	*114*	*535*	**78.69159**
Burn	*348*	*117*	*465*	**25.16129**
Ref. total	*769*	*231*	*1000*	
Producer's %	**54.7464239**	**50.64935**	**Overall %**	**53.8**

VV	Reference Sentinel-2 Moderate High dNBR			
SAR – Sentinel-1	**No burn**	**Burn**	**SAR total**	**User's %**
No burn	*767*	*105*	*872*	**87.95872**
Burn	*71*	*57*	*128*	**44.53125**
Ref. total	*838*	*162*	*1000*	
Producer's %	**91.5274463**	**35.18519**	**Overall %**	**82.4**

VH	Reference Sentinel-2 Moderate High dNBR			
SAR – Sentinel-1	**No burn**	**Burn**	**SAR total**	**User's %**
No burn	456	*79*	*535*	**85.23364**
Burn	*382*	*83*	*465*	**17.84946**
Ref. total	*838*	*162*	*1000*	
Producer's %	**54.4152745**	**51.23457**	**Overall %**	**53.9**

VV	Reference Sentinel-2 High dNBR			
SAR – Sentinel-1	**No burn**	**Burn**	**SAR total**	**User's %**
No burn	*799*	*73*	*872*	**91.62844**
Burn	*83*	*45*	*128*	**35.15625**
Ref. total	*882*	*118*	*1000*	
Producer's %	**90.5895692**	**38.13559**	**Overall %**	**84.4**

VH	Reference Sentinel-2 High dNBR			
SAR – Sentinel-1	**No burn**	**Burn**	**SAR total**	**User's %**
No burn	476	*59*	*535*	**88.97196**
Burn	*406*	*59*	*465*	**12.68817**
Ref. total	*882*	*118*	*1000*	
Producer's %	**53.968254**	**50**	**Overall %**	**53.5**

VV	Reference MODIS Burn			
SAR – Sentinel-1	**No burn**	**Burn**	**SAR total**	**User's %**
No burn	*650*	*222*	*872*	**74.54128**
Burn	*48*	*80*	*128*	**62.5**
Ref. total	*698*	*302*	*1000*	
Producer's %	**93.1232092**	**26.49007**	**Overall %**	**73**

VH	Reference MODIS Burn			
SAR – Sentinel-1	**No burn**	**Burn**	**SAR total**	**User's %**
No burn	383	*152*	*535*	**71.58879**
Burn	*315*	*150*	*465*	**32.25806**
Ref. total	*698*	*302*	*1000*	
Producer's %	**54.8710602**	**49.66887**	**Overall %**	**53.3**

October Ascending

VV	Reference Sentinel-2 Low dNBR			
SAR – Sentinel-1	**No burn**	**Burn**	**SAR total**	**User's %**
No burn	*519*	*188*	*707*	**73.40877**
Burn	*130*	*163*	*293*	**55.6314**
Ref. total	*649*	*351*	*1000*	
Producer's %	**79.9691834**	**46.43875**	**Overall %**	**68.2**

VH	Reference Sentinel-2 Low dNBR			
SAR – Sentinel-1	**No burn**	**Burn**	**SAR total**	**User's %**
No burn	475	*132*	*607*	**78.25371**
Burn	*174*	*219*	*393*	**55.72519**
Ref. total	*649*	*351*	*1000*	
Producer's %	**73.1895223**	**62.39316**	**Overall %**	**69.4**

VV	Reference Sentinel-2 Moderate Low dNBR			
SAR – Sentinel-1	**No burn**	**Burn**	**SAR total**	**User's %**
No burn	*605*	*102*	*707*	**85.57284**
Burn	*171*	*122*	*293*	**41.63823**
Ref. total	*776*	*224*	*1000*	
Producer's %	**77.9639175**	**54.46429**	**Overall %**	**72.7**

VH	Reference Sentinel-2 Moderate Low dNBR			
SAR – Sentinel-1	**No burn**	**Burn**	**SAR total**	**User's %**
No burn	542	*65*	*607*	**89.2916**
Burn	*234*	*159*	*393*	**40.45802**
Ref. total	*776*	*224*	*1000*	
Producer's %	**69.8453608**	**70.98214**	**Overall %**	**70.1**

VV	Reference Sentinel-2 Moderate High dNBR			
SAR – Sentinel-1	**No burn**	**Burn**	**SAR total**	**User's %**
No burn	*643*	*64*	*707*	**90.94767**
Burn	*200*	*93*	*293*	**31.74061**
Ref. total	*843*	*157*	*1000*	
Producer's %	**76.2752076**	**59.23567**	**Overall %**	**73.6**

VH	Reference Sentinel-2 Moderate High dNBR			
SAR – Sentinel-1	**No burn**	**Burn**	**SAR total**	**User's %**
No burn	568	*39*	*607*	**93.57496**
Burn	*275*	*118*	*393*	**30.02545**
Ref. total	*843*	*157*	*1000*	
Producer's %	**67.3784104**	**75.15924**	**Overall %**	**68.6**

VV	Reference Sentinel-2 High dNBR			
SAR – Sentinel-1	**No burn**	**Burn**	**SAR total**	**User's %**
No burn	*668*	*39*	*707*	**94.48373**
Burn	*225*	*68*	*293*	**23.20819**
Ref. total	*893*	*107*	*1000*	
Producer's %	**74.8040314**	**63.5514**	**Overall %**	**73.6**

VH	Reference Sentinel-2 High dNBR			
SAR – Sentinel-1	**No burn**	**Burn**	**SAR total**	**User's %**
No burn	587	*20*	*607*	**96.70511**
Burn	*306*	*87*	*393*	**22.1374**
Ref. total	*893*	*107*	1000	
Producer's %	**65.7334826**	**81.30841**	**Overall %**	**67.4**

VV	Reference MODIS Burn			
SAR – Sentinel-1	**No burn**	**Burn**	**SAR total**	**User's %**
No burn	*551*	*156*	*707*	**77.93494**
Burn	*147*	*146*	*293*	**49.82935**
Ref. total	*698*	*302*	*1000*	
Producer's %	**78.9398281**	**48.34437**	**Overall %**	**69.7**

VH	Reference MODIS Burn			
SAR – Sentinel-1	**No burn**	**Burn**	**SAR total**	**User's %**
No burn	494	*113*	*607*	**81.38386**
Burn	*204*	*189*	*393*	**48.0916**
Ref. total	*698*	*302*	*1000*	
Producer's %	**70.773639**	**62.58278**	**Overall %**	**68.3**

October Descending

VV	Reference Sentinel-2 Low dNBR			
SAR – Sentinel-1	**No burn**	**Burn**	**SAR total**	**User's %**
No burn	*298*	*114*	*412*	**72.3301**
Burn	*351*	*237*	*588*	**40.30612**
Ref. total	*649*	*351*	*1000*	
Producer's %	**45.9167951**	**67.52137**	**Overall %**	**53.5**

VH	Reference Sentinel-2 Low dNBR			
SAR – Sentinel-1	**No burn**	**Burn**	**SAR total**	**User's %**
No burn	207	*86*	*293*	**70.64846**
Burn	*442*	*265*	*707*	**37.48232**
Ref. total	*649*	*351*	*1000*	
Producer's %	**31.8952234**	**75.49858**	**Overall %**	**47.2**

VV	Reference Sentinel-2 Moderate Low dNBR			
SAR – Sentinel-1	**No burn**	**Burn**	**SAR total**	**User's %**
No burn	*346*	*66*	*412*	**83.98058**
Burn	*430*	*158*	*588*	**26.87075**
Ref. total	*776*	*224*	*1000*	
Producer's %	**44.5876289**	**70.53571**	**Overall %**	**50.4**

VH	Reference Sentinel-2 Moderate Low dNBR			
SAR – Sentinel-1	**No burn**	**Burn**	**SAR total**	**User's %**
No burn	254	*39*	*293*	**86.68942**
Burn	*522*	*185*	*707*	**26.1669**
Ref. total	*776*	*224*	*1000*	
Producer's %	**32.7319588**	**82.58929**	**Overall %**	**43.9**

VV	Reference Sentinel-2 Moderate High dNBR			
SAR – Sentinel-1	**No burn**	**Burn**	**SAR total**	**User's %**
No burn	*371*	*41*	*412*	**90.04854**
Burn	*472*	*116*	*588*	**19.72789**
Ref. total	*843*	*157*	*1000*	
Producer's %	**44.0094899**	**73.88535**	**Overall %**	**48.7**

VH	Reference Sentinel-2 Moderate High dNBR			
SAR – Sentinel-1	**No burn**	**Burn**	**SAR total**	**User's %**
No burn	272	*21*	*293*	**92.83276**
Burn	*571*	*136*	*707*	**19.23621**
Ref. total	*843*	*157*	*1000*	
Producer's %	**32.2657177**	**86.6242**	**Overall %**	**40.8**

VV	Reference Sentinel-2 High dNBR			
SAR – Sentinel-1	**No burn**	**Burn**	**SAR total**	**User's %**
No burn	*389*	*23*	*412*	**94.41748**
Burn	*504*	*84*	*588*	**14.28571**
Ref. total	*893*	*107*	*1000*	
Producer's %	**43.5610302**	**78.50467**	**Overall %**	**47.3**

VH	Reference Sentinel-2 High dNBR			
SAR – Sentinel-1	**No burn**	**Burn**	**SAR total**	**User's %**
No burn	282	*11*	*293*	**96.24573**
Burn	*611*	*96*	*707*	**13.5785**
Ref. total	*893*	*107*	1000	
Producer's %	**31.5789474**	**89.71963**	**Overall %**	**37.8**

VV	Reference MODIS Burn			
SAR – Sentinel-1	**No burn**	**Burn**	**SAR total**	**User's %**
No burn	*317*	*95*	*412*	**76.94175**
Burn	*381*	*207*	*588*	**35.20408**
Ref. total	*698*	*302*	*1000*	
Producer's %	**45.4154728**	**68.54305**	**Overall %**	**52.4**

VH	Reference MODIS Burn			
SAR – Sentinel-1	**No burn**	**Burn**	**SAR total**	**User's %**
No burn	221	*72*	*293*	**75.42662**
Burn	*477*	*230*	*707*	**32.53182**
Ref. total	*698*	*302*	*1000*	
Producer's %	**31.6618911**	**76.15894**	**Overall %**	**45.1**

French Fire, California

August Ascending

VV	Reference Sentinel-2 Low dNBR			
SAR – Sentinel-1	**No burn**	**Burn**	**SAR total**	**User's %**
No burn	626	*75*	*701*	**89.3009986**
Burn	*76*	*223*	*299*	**74.5819398**
Ref. total	*702*	*298*	*1000*	
Producer's %	**89.17379**	**74.8322148**	**Overall %**	**84.9**

VH	Reference Sentinel-2 Low dNBR			
SAR – Sentinel-1	**No burn**	**Burn**	**SAR total**	**User's %**
No burn	664	*81*	*745*	**89.1275168**
Burn	*38*	*217*	*255*	**85.0980392**
Ref. total	*702*	*298*	*1000*	
Producer's %	**94.58689**	**72.8187919**	**Overall %**	**88.1**

VV	Reference Sentinel-2 Moderate Low dNBR			
SAR – Sentinel-1	**No burn**	**Burn**	**SAR total**	**User's %**
No burn	670	*31*	*701*	**95.5777461**
Burn	*137*	*162*	*299*	**54.180602**
Ref. total	*807*	*193*	*1000*	
Producer's %	**83.02354**	**83.9378238**	**Overall %**	**83.2**

VH	Reference Sentinel-2 Moderate Low dNBR			
SAR – Sentinel-1	**No burn**	**Burn**	**SAR total**	**User's %**
No burn	713	*32*	*745*	**95.704698**
Burn	*94*	*161*	*255*	**63.1372549**
Ref. total	*807*	*193*	*1000*	
Producer's %	**88.35192**	**83.4196891**	**Overall %**	**87.4**

VV	Reference Sentinel-2 Moderate High dNBR			
SAR – Sentinel-1	**No burn**	**Burn**	**SAR total**	**User's %**
No burn	*685*	*16*	*701*	**97.7175464**
Burn	*188*	*111*	*299*	**37.1237458**
Ref. total	*873*	*127*	*1000*	
Producer's %	**78.46506**	**87.4015748**	**Overall %**	**79.6**

VH	Reference Sentinel-2 Moderate High dNBR			
SAR – Sentinel-1	**No burn**	**Burn**	**SAR total**	**User's %**
No burn	733	*12*	*745*	**98.3892617**
Burn	*140*	*115*	*255*	**45.0980392**
Ref. total	*873*	*127*	*1000*	
Producer's %	**83.96334**	**90.5511811**	**Overall %**	**84.8**

VV	Reference Sentinel-2 High dNBR			
SAR – Sentinel-1	**No burn**	**Burn**	**SAR total**	**User's %**
No burn	*697*	*4*	*701*	**99.4293866**
Burn	*249*	*50*	*299*	**16.722408**
Ref. total	*946*	*54*	*1000*	
Producer's %	**73.67865**	**92.5925926**	**Overall %**	**74.7**

VH	Reference Sentinel-2 High dNBR			
SAR – Sentinel-1	**No burn**	**Burn**	**SAR total**	**User's %**
No burn	743	*2*	*745*	**99.7315436**
Burn	*203*	*52*	*255*	**20.3921569**
Ref. total	*946*	*54*	*1000*	
Producer's %	**78.54123**	**96.2962963**	**Overall %**	**79.5**

VV	Reference MODIS Burn			
SAR – Sentinel-1	**No burn**	**Burn**	**SAR total**	**User's %**
No burn	*596*	*105*	*701*	**85.021398**
Burn	*37*	*262*	*299*	**87.6254181**
Ref. total	*633*	*367*	*1000*	
Producer's %	**94.15482**	**71.389646**	**Overall %**	**85.8**

VH	Reference MODIS Burn			
SAR – Sentinel-1	**No burn**	**Burn**	**SAR total**	**User's %**
No burn	617	*128*	*745*	**82.8187919**
Burn	*16*	*239*	*255*	**93.7254902**
Ref. total	*633*	*367*	*1000*	
Producer's %	**97.47235**	**65.1226158**	**Overall %**	**85.6**

August Descending

VV	Reference Sentinel-2 Low dNBR			
SAR – Sentinel-1	**No burn**	**Burn**	**SAR total**	**User's %**
No burn	*685*	*157*	*842*	**81.3539192**
Burn	*17*	*141*	*158*	**89.2405063**
Ref. total	*702*	*298*	*1000*	
Producer's %	**97.57835**	**47.3154362**	**Overall %**	**82.6**

VH	Reference Sentinel-2 Low dNBR			
SAR – Sentinel-1	**No burn**	**Burn**	**SAR total**	**User's %**
No burn	681	*114*	*795*	**85.6603774**
Burn	*21*	*184*	*205*	**89.7560976**
Ref. total	*702*	*298*	*1000*	
Producer's %	**97.00855**	**61.7449664**	**Overall %**	**86.5**

VV	Reference Sentinel-2 Moderate Low dNBR			
SAR – Sentinel-1	**No burn**	**Burn**	**SAR total**	**User's %**
No burn	*752*	*90*	*842*	**89.3111639**
Burn	*55*	*103*	*158*	**65.1898734**
Ref. total	*807*	*193*	*1000*	
Producer's %	**93.18463**	**53.3678756**	**Overall %**	**85.5**

VH	Reference Sentinel-2 Moderate Low dNBR			
SAR – Sentinel-1	**No burn**	**Burn**	**SAR total**	**User's %**
No burn	737	*58*	*795*	**92.7044025**
Burn	*70*	*135*	*205*	**65.8536585**
Ref. total	*807*	*193*	*1000*	
Producer's %	**91.3259**	**69.9481865**	**Overall %**	**87.2**

VH	Reference Sentinel-2 Moderate Low dNBR			
SAR – Sentinel-1	**No burn**	**Burn**	**SAR total**	**User's %**
No burn	737	*58*	*795*	**92.7044025**
Burn	*70*	*135*	*205*	**65.8536585**
Ref. total	*807*	*193*	*1000*	
Producer's %	**91.3259**	**69.9481865**	**Overall %**	**87.2**

VH	Reference Sentinel-2 Moderate High dNBR			
SAR – Sentinel-1	**No burn**	**Burn**	**SAR total**	**User's %**
No burn	763	*32*	*795*	**95.9748428**
Burn	*110*	*95*	*205*	**46.3414634**
Ref. total	*873*	*127*	*1000*	
Producer's %	**87.39977**	**74.8031496**	**Overall %**	**85.8**

VV	Reference Sentinel-2 High dNBR			
SAR – Sentinel-1	**No burn**	**Burn**	**SAR total**	**User's %**
No burn	*822*	*20*	*842*	**97.6247031**
Burn	*124*	*34*	*158*	**21.5189873**
Ref. total	*946*	*54*	*1000*	
Producer's %	**86.89218**	**62.962963**	**Overall %**	**85.6**

VH	Reference Sentinel-2 High dNBR			
SAR – Sentinel-1	**No burn**	**Burn**	**SAR total**	**User's %**
No burn	784	*11*	*795*	**98.6163522**
Burn	*162*	*43*	*205*	**20.9756098**
Ref. total	*946*	*54*	*1000*	
Producer's %	**82.87526**	**79.6296296**	**Overall %**	**82.7**

VV	Reference MODIS Burn			
SAR – Sentinel-1	**No burn**	**Burn**	**SAR total**	**User's %**
No burn	626	216	*842*	**74.3467933**
Burn	7	151	*158*	**95.5696203**
Ref. total	*633*	*367*	*1000*	
Producer's %	**98.89415**	**41.1444142**	**Overall %**	**77.7**

VH	Reference MODIS Burn			
SAR – Sentinel-1	**No burn**	**Burn**	**SAR total**	**User's %**
No burn	623	172	*795*	**78.3647799**
Burn	10	195	*205*	**95.1219512**
Ref. total	*633*	*367*	*1000*	
Producer's %	**98.42022**	**53.133515**	**Overall %**	**81.8**

September Ascending

VV	Reference Sentinel-2 Low dNBR			
SAR – Sentinel-1	**No burn**	**Burn**	**SAR total**	**User's %**
No burn	540	*97*	*637*	**84.7723705**
Burn	*93*	*270*	*363*	**74.3801653**
Ref. total	*633*	*367*	*1000*	
Producer's %	**85.30806**	**73.5694823**	**Overall %**	**81**

VH	Reference Sentinel-2 Low dNBR			
SAR – Sentinel-1	**No burn**	**Burn**	**SAR total**	**User's %**
No burn	574	*104*	*678*	**84.660767**
Burn	*59*	*263*	*322*	**81.6770186**
Ref. total	*633*	*367*	*1000*	
Producer's %	**90.6793**	**71.6621253**	**Overall %**	**83.7**

VV	Reference Sentinel-2 Moderate Low dNBR			
SAR – Sentinel-1	**No burn**	**Burn**	**SAR total**	**User's %**
No burn	590	*47*	*637*	**92.6216641**
Burn	*148*	*215*	*363*	**59.2286501**
Ref. total	*738*	*262*	*1000*	
Producer's %	**79.9458**	**82.0610687**	**Overall %**	**80.5**

VH	Reference Sentinel-2 Moderate Low dNBR			
SAR – Sentinel-1	**No burn**	**Burn**	**SAR total**	**User's %**
No burn	630	*48*	*678*	**92.920354**
Burn	*108*	*214*	*322*	**66.4596273**
Ref. total	*738*	*262*	*1000*	
Producer's %	**85.36585**	**81.6793893**	**Overall %**	**84.4**

VV	Reference Sentinel-2 Moderate High dNBR			
SAR – Sentinel-1	**No burn**	**Burn**	**SAR total**	**User's %**
No burn	*615*	*22*	*637*	**96.5463108**
Burn	*233*	*130*	*363*	**35.8126722**
Ref. total	*848*	*152*	*1000*	
Producer's %	**72.52358**	**85.5263158**	**Overall %**	**74.5**

VH	Reference Sentinel-2 Moderate High dNBR			
SAR – Sentinel-1	**No burn**	**Burn**	**SAR total**	**User's %**
No burn	660	*18*	*678*	**97.3451327**
Burn	*188*	*134*	*322*	**41.6149068**
Ref. total	*848*	*152*	*1000*	
Producer's %	**77.83019**	**88.1578947**	**Overall %**	**79.4**

VV	Reference Sentinel-2 High dNBR			
SAR – Sentinel-1	**No burn**	**Burn**	**SAR total**	**User's %**
No burn	*631*	*6*	*637*	**99.0580848**
Burn	*287*	*76*	*363*	**20.9366391**
Ref. total	*918*	*82*	*1000*	
Producer's %	**68.73638**	**92.6829268**	**Overall %**	**70.7**

VH	Reference Sentinel-2 High dNBR			
SAR – Sentinel-1	**No burn**	**Burn**	**SAR total**	**User's %**
No burn	673	*5*	*678*	**99.2625369**
Burn	*245*	*77*	*322*	**23.9130435**
Ref. total	*918*	*82*	*1000*	
Producer's %	**73.31155**	**93.902439**	**Overall %**	**75**

VV	Reference MODIS Burn			
SAR – Sentinel-1	**No burn**	**Burn**	**SAR total**	**User's %**
No burn	*523*	*114*	*637*	**82.1036107**
Burn	*76*	*287*	*363*	**79.0633609**
Ref. total	*599*	*401*	*1000*	
Producer's %	**87.31219**	**71.5710723**	**Overall %**	**81**

VH	Reference MODIS Burn			
SAR – Sentinel-1	**No burn**	**Burn**	**SAR total**	**User's %**
No burn	550	*128*	*678*	**81.120944**
Burn	*49*	*273*	*322*	**84.7826087**
Ref. total	*599*	*401*	*1000*	
Producer's %	**91.8197**	**68.0798005**	**Overall %**	**82.3**

September Descending

VV	Reference Sentinel-2 Low dNBR			
SAR – Sentinel-1	**No burn**	**Burn**	**SAR total**	**User's %**
No burn	*613*	*265*	*878*	**69.8177677**
Burn	*20*	*102*	*122*	**83.6065574**
Ref. total	*633*	*367*	*1000*	
Producer's %	**96.84044**	**27.7929155**	**Overall %**	**71.5**

VH	Reference Sentinel-2 Low dNBR			
SAR – Sentinel-1	**No burn**	**Burn**	**SAR total**	**User's %**
No burn	437	*129*	*566*	**77.2084806**
Burn	*196*	*238*	*434*	**54.8387097**
Ref. total	*633*	*367*	*1000*	
Producer's %	**69.03633**	**64.8501362**	**Overall %**	**67.5**

VV	Reference Sentinel-2 Moderate Low dNBR			
SAR – Sentinel-1	**No burn**	**Burn**	**SAR total**	**User's %**
No burn	*707*	*171*	*878*	**80.523918**
Burn	*31*	*91*	*122*	**74.5901639**
Ref. total	*738*	*262*	*1000*	
Producer's %	**95.79946**	**34.7328244**	**Overall %**	**79.8**

VH	Reference Sentinel-2 Moderate Low dNBR			
SAR – Sentinel-1	**No burn**	**Burn**	**SAR total**	**User's %**
No burn	496	*70*	*566*	**87.6325088**
Burn	*242*	*192*	*434*	**44.2396313**
Ref. total	*738*	*262*	*1000*	
Producer's %	**67.20867**	**73.2824427**	**Overall %**	**68.8**

VV	Reference Sentinel-2 Moderate High dNBR			
SAR – Sentinel-1	**No burn**	**Burn**	**SAR total**	**User's %**
No burn	*783*	*95*	*878*	**89.1799544**
Burn	*65*	*57*	*122*	**46.7213115**
Ref. total	*848*	*152*	*1000*	
Producer's %	**92.33491**	**37.5**	**Overall %**	**84**

VH	Reference Sentinel-2 Moderate High dNBR			
SAR – Sentinel-1	**No burn**	**Burn**	**SAR total**	**User's %**
No burn	534	*32*	*566*	**94.3462898**
Burn	*314*	*120*	*434*	**27.6497696**
Ref. total	*848*	*152*	*1000*	
Producer's %	**62.9717**	**78.9473684**	**Overall %**	**65.4**

VV	Reference Sentinel-2 High dNBR			
SAR – Sentinel-1	**No burn**	**Burn**	**SAR total**	**User's %**
No burn	*830*	*48*	*878*	**94.5330296**
Burn	*88*	*34*	*122*	**27.8688525**
Ref. total	*918*	*82*	*1000*	
Producer's %	**90.41394**	**41.4634146**	**Overall %**	**86.4**

VH	Reference Sentinel-2 High dNBR			
SAR – Sentinel-1	**No burn**	**Burn**	**SAR total**	**User's %**
No burn	555	*11*	*566*	**98.0565371**
Burn	*363*	*71*	*434*	**16.359447**
Ref. total	*918*	*82*	*1000*	
Producer's %	**60.45752**	**86.5853659**	**Overall %**	**62.6**

VV	Reference MODIS Burn			
SAR – Sentinel-1	**No burn**	**Burn**	**SAR total**	**User's %**
No burn	*579*	*299*	*878*	**65.9453303**
Burn	*20*	*102*	*122*	**83.6065574**
Ref. total	*599*	*401*	*1000*	
Producer's %	**96.6611**	**25.436409**	**Overall %**	**68.1**

VH	Reference MODIS Burn			
SAR – Sentinel-1	**No burn**	**Burn**	**SAR total**	**User's %**
No burn	420	*146*	*566*	**74.204947**
Burn	*179*	*255*	*434*	**58.7557604**
Ref. total	*599*	*401*	*1000*	
Producer's %	**70.11686**	**63.5910224**	**Overall %**	**67.5**

October Ascending

VV	Reference Sentinel-2 Low dNBR			
SAR – Sentinel-1	**No burn**	**Burn**	**SAR total**	**User's %**
No burn	368	*244*	*612*	**60.130719**
Burn	*225*	*163*	*388*	**42.0103093**
Ref. total	*593*	*407*	*1000*	
Producer's %	**62.05734**	**40.04914**	**Overall %**	**53.1**

VH	Reference Sentinel-2 Low dNBR			
SAR – Sentinel-1	**No burn**	**Burn**	**SAR total**	**User's %**
No burn	495	*242*	*737*	**67.1641791**
Burn	*98*	*165*	*263*	**62.7376426**
Ref. total	*593*	*407*	*1000*	
Producer's %	**83.47386**	**40.5405405**	**Overall %**	**66**

VV	Reference Sentinel-2 Moderate Low dNBR			
SAR – Sentinel-1	**No burn**	**Burn**	**SAR total**	**User's %**
No burn	464	*148*	*612*	**75.8169935**
Burn	*270*	*118*	*388*	**30.4123711**
Ref. total	*734*	*266*	*1000*	
Producer's %	**63.21526**	**44.3609023**	**Overall %**	**58.2**

VH	Reference Sentinel-2 Moderate Low dNBR			
SAR – Sentinel-1	**No burn**	**Burn**	**SAR total**	**User's %**
No burn	601	*136*	*737*	**81.5468114**
Burn	*133*	*130*	*263*	**49.4296578**
Ref. total	*734*	*266*	*1000*	
Producer's %	**81.88011**	**48.8721805**	**Overall %**	**73.1**

VV	Reference Sentinel-2 Moderate High dNBR			
SAR – Sentinel-1	**No burn**	**Burn**	**SAR total**	**User's %**
No burn	*528*	*84*	*612*	**86.2745098**
Burn	*304*	*84*	*388*	**21.6494845**
Ref. total	*832*	*168*	*1000*	
Producer's %	**63.46154**	**50**	**Overall %**	**61.2**

VH	Reference Sentinel-2 Moderate High dNBR			
SAR – Sentinel-1	**No burn**	**Burn**	**SAR total**	**User's %**
No burn	654	*83*	*737*	**88.7381275**
Burn	*178*	*85*	*263*	**32.3193916**
Ref. total	*832*	*168*	*1000*	
Producer's %	**78.60577**	**50.5952381**	**Overall %**	**73.9**

VV	Reference Sentinel-2 High dNBR			
SAR – Sentinel-1	**No burn**	**Burn**	**SAR total**	**User's %**
No burn	*561*	*51*	*612*	**91.6666667**
Burn	*340*	*48*	*388*	**12.371134**
Ref. total	*901*	*99*	*1000*	
Producer's %	**62.26415**	**48.4848485**	**Overall %**	**60.9**

VH	Reference Sentinel-2 High dNBR			
SAR – Sentinel-1	**No burn**	**Burn**	**SAR total**	**User's %**
No burn	687	*50*	*737*	**93.2157395**
Burn	*214*	*49*	*263*	**18.6311787**
Ref. total	*901*	*99*	*1000*	
Producer's %	**76.24861**	**49.4949495**	**Overall %**	**73.6**

VH	Reference Sentinel-2 High dNBR			
SAR – Sentinel-1	**No burn**	**Burn**	**SAR total**	**User's %**
No burn	687	*50*	*737*	**93.2157395**
Burn	*214*	*49*	*263*	**18.6311787**
Ref. total	*901*	*99*	*1000*	
Producer's %	**76.24861**	**49.4949495**	**Overall %**	**73.6**

VH	Reference MODIS Burn			
SAR – Sentinel-1	**No burn**	**Burn**	**SAR total**	**User's %**
No burn	506	*231*	*737*	**68.6567164**
Burn	*93*	*170*	*263*	**64.6387833**
Ref. total	*599*	*401*	*1000*	
Producer's %	**84.47412**	**42.394015**	**Overall %**	**67.6**

October Descending

VV	Reference Sentinel-2 Low dNBR			
SAR – Sentinel-1	**No burn**	**Burn**	**SAR total**	**User's %**
No burn	*370*	*241*	*611*	**60.5564648**
Burn	*223*	*166*	*389*	**42.6735219**
Ref. total	*593*	*407*	*1000*	
Producer's %	**62.3946**	**40.7862408**	**Overall %**	**53.6**

VV	Reference Sentinel-2 Low dNBR			
SAR – Sentinel-1	**No burn**	**Burn**	**SAR total**	**User's %**
No burn	*370*	*241*	*611*	**60.5564648**
Burn	*223*	*166*	*389*	**42.6735219**
Ref. total	*593*	*407*	*1000*	
Producer's %	**62.3946**	**40.7862408**	**Overall %**	**53.6**

VV	Reference Sentinel-2 Low dNBR			
SAR – Sentinel-1	**No burn**	**Burn**	**SAR total**	**User's %**
No burn	*370*	*241*	*611*	**60.5564648**
Burn	*223*	*166*	*389*	**42.6735219**
Ref. total	*593*	*407*	*1000*	
Producer's %	**62.3946**	**40.7862408**	**Overall %**	**53.6**

VH	Reference Sentinel-2 Moderate Low dNBR			
SAR – Sentinel-1	**No burn**	**Burn**	**SAR total**	**User's %**
No burn	394	*146*	*540*	**72.962963**
Burn	*340*	*120*	*460*	**26.0869565**
Ref. total	*734*	*266*	*1000*	
Producer's %	**53.67847**	**45.112782**	**Overall %**	**51.4**

VV	Reference Sentinel-2 Moderate High dNBR			
SAR – Sentinel-1	**No burn**	**Burn**	**SAR total**	**User's %**
No burn	*512*	*99*	*611*	**83.797054**
Burn	*320*	*69*	*389*	**17.7377892**
Ref. total	*832*	*168*	*1000*	
Producer's %	**61.53846**	**41.0714286**	**Overall %**	**58.1**

VH	Reference Sentinel-2 Moderate High dNBR			
SAR – Sentinel-1	**No burn**	**Burn**	**SAR total**	**User's %**
No burn	439	*101*	*540*	**81.2962963**
Burn	*393*	*67*	*460*	**14.5652174**
Ref. total	*832*	*168*	*1000*	
Producer's %	**52.76442**	**39.8809524**	**Overall %**	**50.6**

VH	Reference Sentinel-2 Moderate High dNBR			
SAR – Sentinel-1	**No burn**	**Burn**	**SAR total**	**User's %**
No burn	439	*101*	*540*	**81.2962963**
Burn	*393*	*67*	*460*	**14.5652174**
Ref. total	*832*	*168*	*1000*	
Producer's %	**52.76442**	**39.8809524**	**Overall %**	**50.6**

VH	Reference Sentinel-2 High dNBR			
SAR – Sentinel-1	**No burn**	**Burn**	**SAR total**	**User's %**
No burn	480	*60*	*540*	**88.8888889**
Burn	*421*	*39*	*460*	**8.47826087**
Ref. total	*901*	*99*	*1000*	
Producer's %	**53.27414**	**39.3939394**	**Overall %**	**51.9**

VV	Reference MODIS Burn			
SAR – Sentinel-1	**No burn**	**Burn**	**SAR total**	**User's %**
No burn	*368*	*243*	*611*	**60.2291326**
Burn	*231*	*158*	*389*	**40.6169666**
Ref. total	*599*	*401*	*1000*	
Producer's %	**61.43573**	**39.4014963**	**Overall %**	**52.6**

VH	Reference MODIS Burn			
SAR – Sentinel-1	**No burn**	**Burn**	**SAR total**	**User's %**
No burn	326	*214*	*540*	**60.3703704**
Burn	*273*	*187*	*460*	**40.6521739**
Ref. total	*599*	*401*	*1000*	
Producer's %	**54.42404**	**46.6334165**	**Overall %**	**51.3**

REFERENCES

Abatzoglou, John T., and A. Park Williams. “Impact of Anthropogenic Climate Change on Wildfire across Western US Forests.” *Proceedings of the National Academy of Sciences*, vol. 113, no. 42, Oct. 2016, pp. 11770–75, doi:10.1073/pnas.1607171113.

Ager, Alan A., et al. “Wildfire Exposure to the Wildland Urban Interface in the Western US.” *Applied Geography*, vol. 111, Oct. 2019, p. 102059, doi:10.1016/j.apgeog.2019.102059.

Ajadi, Olaniyi A., et al. “Change Detection in Synthetic Aperture Radar Images Using a Multiscale-Driven Approach.” *Remote Sensing*, vol. 8, no. 6, June 2016, p. 482, doi:10.3390/rs8060482.

Andela, N., et al. “A Human-Driven Decline in Global Burned Area.” *Science*, vol. 356, no. 6345, June 2017, pp. 1356–62, https://doi.org/10.1126/science.aal4108.

Ban, Yifang, et al. “Near Real-Time Wildfire Progression Monitoring with Sentinel-1 SAR Time Series and Deep Learning.” *Scientific Reports*, vol. 10, no. 1, Jan. 2020, p. 1322, https://doi.org/10.1038/s41598-019-56967-x.

Baldassari, Erin. “Camp Fire Death Toll Grows to 29, Matching 1933 Blaze as State’s Deadliest.” *East Bay Times*, 11 Nov. 2018, https://www.mercurynews.com/crews-continue-to-battle-strong-winds-in-deadly-camp-fire.

Celik, Turgay. “Unsupervised Change Detection in Satellite Images Using Principal Component Analysis and k-Means Clustering.” *IEEE Geoscience and Remote Sensing Letters*, vol. 6, no. 4, Oct. 2009, pp. 772–76, https://doi.org/10.1109/LGRS.2009.2025059.

Cook, Benjamin I., et al. “Unprecedented 21st Century Drought Risk in the American Southwest and Central Plains.” *Science Advances*, Feb. 2015, doi:10.1126/sciadv.1400082. world.

Cocke, Allison E., et al. “Comparison of Burn Severity Assessments Using Differenced Normalized Burn Ratio and Ground Data.” *International Journal of Wildland Fire*, vol. 14, no. 2, June 2005, pp. 189–98, doi:10.1071/WF04010.

CNBC, “Deadly California Wildfire Now 100% Contained after Scorching 154,000 Acres.” *CNBC*, 25 Nov. 2018, https://www.cnbc.com/2018/11/25/deadly-california-wildfire-now-100percent-contained.html.

European Space Agency, ESA. *“Sentinel-1 Technical Guide.”* 2012

Fletcher, Karen, and European Space Agency, editors. *Sentinel-1: ESA’s Radar Observatory Mission for GMES Operational Services*. ESA Communications, 2012.

Gao, Peng, et al. “Robust Projections of Future Fire Probability for the Conterminous United States.” *Science of The Total Environment*, vol. 789, Oct. 2021, p. 147872, doi:10.1016/j.scitotenv.2021.147872.

García, M. J. López, and V. Caselles. “Mapping Burns and Natural Reforestation Using Thematic Mapper Data.” *Geocarto International*, vol. 6, no. 1, 1991, pp. 31–37, https://doi.org/10.1080/10106049109354290.

Giglio, L., C. Justice, L. Boschetti, D. Roy. *MODIS/Terra+Aqua Burned Area Monthly L3 Global 500m SIN Grid V061* 2021, distributed by NASA EOSDIS Land Processes DAAC, https://doi.org/10.5067/MODIS/MCD64A1.061.

Gorelick, Noel, et al. “Google Earth Engine: Planetary-Scale Geospatial Analysis for Everyone.” *Remote Sensing of Environment*, vol. 202, Dec. 2017, pp. 18–27, doi:10.1016/j.rse.2017.06.031.

Halofsky, Jessica E., et al. “Changing Wildfire, Changing Forests: The Effects of Climate Change on Fire Regimes and Vegetation in the Pacific Northwest, USA.” *Fire Ecology*, vol. 16, no. 1, Jan. 2020, p. 4, doi:10.1186/s42408-019-0062-8.

Heidari, Hadi, et al. “Effects of Climate Change on Natural-Caused Fire Activity in Western U.S. National Forests.” *Atmosphere*, vol. 12, no. 8, July 2021, p. 981, doi:10.3390/atmos12080981.

Hird, Jennifer N., et al. “Google Earth Engine, Open-Access Satellite Data, and Machine Learning in Support of Large-Area Probabilistic Wetland Mapping.” *Remote Sensing*, vol. 9, no. 12, Dec. 2017, p. 1315, https://doi.org/10.3390/rs9121315.

Hoekman, Dirk H., and Johannes Reiche. “Multi-Model Radiometric Slope Correction of SAR Images of Complex Terrain Using a Two-Stage Semi-Empirical Approach.” *Remote Sensing of Environment*, vol. 156, Jan. 2015, pp. 1–10, https://doi.org/10.1016/j.rse.2014.08.037.

Imperatore, Pasquale, et al. "Effect of the Vegetation Fire on Backscattering: An Investigation Based on Sentinel-1 Observations." *IEEE Journal of Selected Topics in Applied Earth Observations and Remote Sensing*, vol. 10, no. 10, Oct. 2017, pp. 4478–92, doi:10.1109/JSTARS.2017.2717039.

Jolly, W. Matt, et al. "Climate-Induced Variations in Global Wildfire Danger from 1979 to 2013." *Nature Communications*, vol. 6, no. 1, July 2015, p. 7537, https://doi.org/10.1038/ncomms8537.

Kasischke, Eric S., et al. "Monitoring of Wildfires in Boreal Forests Using Large Area AVHRR NDVI Composite Image Data." *Remote Sensing of Environment*, vol. 45, no. 1, July 1993, pp. 61–71, https://doi.org/10.1016/0034-4257(93)90082-9.

Keeton, William S., et al. "Chapter 13 Climate Variability, Climate Change, and Western Wildfire with Implications for the Urban–Wildland Interface." *Living on the Edge*, edited by Austin Troy and Roger G. Kennedy, vol. 6, Emerald Group Publishing Limited, 2007, pp. 225–53, doi:10.1016/S1569-3740(06)06013-5.

Key, Carl H., and Nathan C. Benson. "Landscape Assessment (LA)." In: Lutes, Duncan C.; Keane, Robert E.; Caratti, John F.; Key, Carl H.; Benson, Nathan C.; Sutherland, Steve; Gangi, Larry J. 2006. FIREMON: Fire Effects Monitoring and Inventory System. Gen. Tech. Rep. RMRS-GTR-164-CD. Fort Collins, CO: U.S. Department of Agriculture, Forest Service, Rocky Mountain Research Station. p. LA-1-55, vol. 164, 2006, http://www.fs.usda.gov/treesearch/pubs/24066.

Lasaponara, Rosa, and Biagio Tucci. "Identification of Burned Areas and Severity Using SAR Sentinel-1." *IEEE Geoscience and Remote Sensing Letters*, vol. 16, no. 6, June 2019, pp. 917–21, https://doi.org/10.1109/LGRS.2018.2888641.

Lee, Jaese, et al. "Detection of Forest Fire Damage from Sentinel-1 SAR Data through the Synergistic Use of Principal Component Analysis and K-means Clustering." *Korean Journal of Remote Sensing*, vol. 37, no. 5_3, 2021, pp. 1373–87, https://doi.org/10.7780/kjrs.2021.37.5.3.4.

Liew, S. C., et al. "Delineating Land/Forest Fire Burnt Scars with ERS Interferometric Synthetic Aperture Radar." *Geophysical Research Letters*, vol. 26, no. 16, 1999, pp. 2409–12, https://doi.org/10.1029/1999GL900189.

Littell, Jeremy S., et al. "A Review of the Relationships between Drought and Forest Fire in the United States." *Global Change Biology*, vol. 22, no. 7, 2016, pp. 2353–69, https://doi.org/10.1111/gcb.13275.

Loew, Alexander, and Wolfram Mauser. “Generation of Geometrically and Radiometrically Terrain Corrected SAR Image Products.” *Remote Sensing of Environment*, vol. 106, no. 3, Feb. 2007, pp. 337–49, https://doi.org/10.1016/j.rse.2006.09.002.

McKenzie, Donald, and Jeremy S. Littell. “Climate Change and the Eco-hydrology of Fire: Will Area Burned Increase in a Warming Western USA?” *Ecological Applications*, vol. 27, no. 1, 2017, pp. 26–36, https://doi.org/10.1002/eap.1420.

Mullissa, Adugna, et al. “Sentinel-1 SAR Backscatter Analysis Ready Data Preparation in Google Earth Engine.” *Remote Sensing*, vol. 13, no. 10, Jan. 2021, p. 1954, doi:10.3390/rs13101954.

Parks, S. A., and J. T. Abatzoglou. “Warmer and Drier Fire Seasons Contribute to Increases in Area Burned at High Severity in Western US Forests From 1985 to 2017.” *Geophysical Research Letters*, vol. 47, no. 22, 2020, p. e2020GL089858, doi:10.1029/2020GL089858.

Salvador, R., et al. “A Semi-Automatic Methodology to Detect Fire Scars in Shrubs and Evergreen Forests with Landsat MSS Time Series.” *International Journal of Remote Sensing*, vol. 21, no. 4, Jan. 2000, pp. 655–71, https://doi.org/10.1080/014311600210498.

Schwartz, Mark D. “Green-Wave Phenology.” *Nature*, vol. 394, no. 6696, Aug. 1998, pp. 839–40, doi:10.1038/29670.

Small, David. “Flattening Gamma: Radiometric Terrain Correction for SAR Imagery.” *IEEE Transactions on Geoscience and Remote Sensing*, vol. 49, no. 8, Aug. 2011, pp. 3081–93, https://doi.org/10.1109/TGRS.2011.2120616.

Steele-Dunne, Susan C., et al. “Radar Remote Sensing of Agricultural Canopies: A Review.” *IEEE Journal of Selected Topics in Applied Earth Observations and Remote Sensing*, vol. 10, no. 5, 2017, pp. 2249–73, doi:10.1109/JSTARS.2016.2639043.

Tanase, Mihai A., et al. “Properties of X-, C- and L-Band Repeat-Pass Interferometric SAR Coherence in Mediterranean Pine Forests Affected by Fires.” *Remote Sensing of Environment*, vol. 114, no. 10, Oct. 2010, pp. 2182–94, doi:10.1016/j.rse.2010.04.021.

Trenberth, Kevin E. “Changes in Precipitation with Climate Change.” *Climate Research*, vol. 47, no. 1–2, Mar. 2011, pp. 123–38, doi:10.3354/cr00953.

Verhegghen, Astrid, et al. “The Potential of Sentinel Satellites for Burnt Area Mapping and Monitoring in the Congo Basin Forests.” *Remote Sensing*, vol. 8, no. 12, Nov. 2016, p. 986, https://doi.org/10.3390/rs8120986.

Viedma, O., et al. “Modeling Rates of Ecosystem Recovery after Fires by Using Landsat TM Data.” *Remote Sensing of Environment*, vol. 61, no. 3, Sept. 1997, pp. 383–98, https://doi.org/10.1016/S0034-4257(97)00048-5.

Vollrath, Andreas, et al. “Angular-Based Radiometric Slope Correction for Sentinel-1 on Google Earth Engine.” *Remote Sensing*, vol. 12, no. 11, Jan. 2020, p. 1867, https://doi.org/10.3390/rs12111867.

Williams, A. Park, et al. “Observed Impacts of Anthropogenic Climate Change on Wildfire in California.” *Earth’s Future*, vol. 7, no. 8, 2019, pp. 892–910, doi:10.1029/2019EF001210.

Westerling, Anthony LeRoy. “Increasing Western US Forest Wildfire Activity: Sensitivity to Changes in the Timing of Spring.” *Philosophical Transactions of the Royal Society B: Biological Sciences*, vol. 371, no. 1696, June 2016, p. 20150178, doi:10.1098/rstb.2015.0178.

Zhang, Puzhao, et al. “An Implicit Radar Convolutional Burn Index for Burnt Area Mapping with Sentinel-1 C-Band SAR Data.” *ISPRS Journal of Photogrammetry and Remote Sensing*, vol. 158, Dec. 2019, pp. 50–62, https://doi.org/10.1016/j.isprsjprs.2019.09.013.

Zhang, Puzhao, et al. “Learning U-Net without Forgetting for near Real-Time Wildfire Monitoring by the Fusion of SAR and Optical Time Series.” *Remote Sensing of Environment*, vol. 261, Aug. 2021, p. 112467, https://doi.org/10.1016/j.rse.2021.112467.

BIOGRAPHY

Louis D. Heying received his Bachelor of Science in Geography and Environmental Planning from Towson University in 2014. After receiving his Master of Science in Earth Systems Science from George Mason University in 2023, he will continue his career with the federal government.